The Cardioprotective Role of NACA in the Prevention of Doxorubicin and Trastuzumab Mediated Cardiac Dysfunction

By

Vineet Goyal

A thesis submitted to the faulty of Graduate Studies of

The University of Manitoba

In partial fulfillment of the requirements

Of the degree of

Master of Science

Department of Physiology and Pathophysiology

College of Medicine, Faculty of Health Sciences

University of Manitoba

Winnipeg, Manitoba, Canada

Abstract

Background: Anthracycline therapy with Doxorubicin (DOX) is very effective in combatting breast cancer, but its clinical use is limited due to its inherent cardiotoxic side effects. The recent introduction of Trastuzumab (TRZ), which is a monoclonal antibody against the human epidermal growth factor receptor known as HER-2, in the breast cancer setting is known to potentiate the effects of DOX mediated cardiac dysfunction. Given the severity of this drug-induced cardiomyopathy, the potential use of prophylactic antioxidants to attenuate the effects of DOX+TRZ mediated cardiac dysfunction has gained recent attention.

Objective: To investigate whether the anti-oxidant, N-acetylcysteine amide (NACA), can attenuate the drug-induced heart failure caused by Doxorubicin and Trastuzumab (DOX+TRZ).

Methods: A total of 100 C57Bl/6 female mice received one of the following drug regimens: i) Saline; ii) NACA; iii) DOX; iv) TRZ; v) DOX+TRZ; vi) NACA+DOX; vii) NACA+TRZ; and viii) NACA+DOX+TRZ. Serial cardiac function was assessed using echocardiography. At day 10, mice were euthanized and hearts were analyzed for oxidative stress (OS) and apoptosis.

Results: In mice receiving DOX, left ventricular ejection fraction (LVEF) decreased from 73±4% to 43±2% at day 10. In mice receiving DOX+TRZ, LVEF decreased from 72±3% to 32±2% at day 10. Prophylactic administration of NACA to mice receiving DOX or DOX+TRZ was cardio-protective with an LVEF of 62±3% and 55±3% at day 10, respectively. In addition, the histological damage observed in DOX+TRZ treated

mice by electron microscopy, was also attenuated by prophylactic NACA administration. Additionally, there was a 3-fold and 4-fold increase in superoxide production in mice treated with DOX or DOX+TRZ at day 10, respectively, which was also attenuated by the prophylactic administration of NACA. Similarly, although the degree of oxidized phospholipids was increased in mice receiving DOX or DOX+TRZ, the prophylactic administration of NACA attenuated the degree of OS in both groups. Finally, there was a 1.5-fold and 2 fold increase in the Bax/Bcl-xL ratio in hearts of mice treated with DOX or DOX+TRZ, respectively. Prophylactic administration of NACA attenuated the degree of apoptosis in both groups.

Conclusion: NACA attenuates the cardiotoxic side effects of DOX+TRZ in a murine model of chemotherapy induced cardiac dysfunction by decreasing OS and apoptosis.

Acknowledgements

Firstly, I owe my deepest gratitude to my supervisors, Dr. Davinder S. Jassal and Dr. Pawan K. Singal, for their continued guidance, support, and expertise throughout my time at the Institute of Cardiovascular Sciences, St. Boniface Research Center. Thank you both for all of your mentorship and helping me build the foundation I needed to pursue my future career goals. Your efforts have made me a better student, and I am forever grateful for that. I would also like to thank my committee members, Dr. Jeff Wigle, Dr. Amir Ravandi, and Dr. Elissavet Kardami for your time, mentorship, and continued support. I would also like to specially thank Dr. James Thliveris for all of his efforts and expertise in electron microscopy. Finally, Dr. Naranjan S. Dhalla, thank you for your encouraging words and teachings in cardiac physiology.

To the members of the Cardiovascular Imaging Laboratory, I would like to thank you for your help over the past 2 years. I would like to thank Ms. Sheena Premecz for all her help with cardiac imaging and project planning. A special thanks to Mr. David Cheung, not only for all of his help in western blotting and qPCR, but also for being a great colleague and a dear friend. To the members of the Cell Pathophysiology Laboratory, I would like to thank you for all of discussions and insight you have provided me with. Specifically, I would like to show my gratitude and thanks to Mrs. Soma Mandal for all of her time and patience with teaching me western blotting and qPCR.

All of this of course would not have been possible without the support of my family. I am grateful to have such supportive parents, my father Surinder, and

mother Vijay, who have always been supportive during my education. I would also like to thank my brother Vishal who has always been supportive and encouraging of any endeavor I have chosen to pursue.

Table of Contents

List of Figures

Figure 7: A total of 70 WT C57Bl/6 female mice were randomized to one of the following drug regimens : Saline; NACA; DOX; TRZ; DOX+TRZ; NACA+DOX; NACA+TRZ; and NACA+DOX+TRZ. NACA was administered 30 minutes prior to the experimental arm. Following injection with one of the above drug regimens, the mice were euthanized at 72 hours to allow an early time point for biochemical analysis.

Figure 8: The LVEDD of groups of wild type C57Bl/6 female mice at day 10. In wild type mice receiving saline, there was no significant difference in LVEDD at baseline and 10 days of follow-up. In WT female mice receiving DOX alone, LVEDD increased from 3.2±0.2 at baseline to 3.9±0.2 at day 10 ($p<0.05$). In WT female mice receiving the combination of DOX+TRZ, LVEDD increased from 3.2±0.1 at baseline to 4.3±0.2 at day 10 ($p<0.05$). Prophylactic administration of NACA to WT female mice receiving either DOX alone or DOX+TRZ was cardioprotective with an LVEDD of 3.4±0.1and 3.6±0.1 at day 10 ($p<0.05$), respectively.

* $p<0.05$ Saline vs DOX

** $p<0.05$ Saline vs DOX+TRZ and DOX vs DOX+TRZ

# $p<0.05$ DOX VS NACA+DOX

$p<0.05$ DOX+TRZ vs NACA+DOX+TRZ and NACA+DOX vs NACA+DOX+TRZ

Figure 9: The LVEF of groups of wild type C57Bl/6 female mice at day 10. In wild type mice receiving either saline or TRZ alone, there was no significant difference in LVEF at baseline and 10 days of follow-up. In WT female mice receiving DOX alone, LVEF decreased from 75±2% at baseline to 43±2% at day 10 ($p<0.05$). In WT female mice receiving the combination of DOX+TRZ, LVEF decreased from 75±3% at baseline to 32±2% at day 10 ($p<0.05$). Prophylactic administration of NACA to WT female mice receiving either DOX alone or DOX+TRZ was cardioprotective with an LVEF of 62±3% and 55±3% at day 10 ($p<0.05$), respectively.

* $p<0.05$ Saline vs DOX

** $p<0.05$ Saline vs DOX+TRZ and DOX vs DOX+TRZ

# $p<0.05$ DOX VS NACA+DOX

p<0.05 DOX+TRZ vs NACA+DOX+TRZ and NACA+DOX vs NACA+DOX+TRZ

Figure 10: Cytoskeletal protein analysis in C57Bl/6 female mice at day 10. Treatment groups include Saline (n=2), NACA (n=2), DOX+HER (n=5), and NACA+DOX+HER (n=5). No significant changes were observed between the various treatment arms at day 10 in any of the groups.

Figure 11: A total of 25 WT female mice (n=5 per group) were treated with either 0.9% saline, DOX, DOX + TRZ, NACA + DOX, or NACA+DOX+TRZ. NACA injections were administered 30 minutes prior to the experimental arm. Cardiac tissue was harvested at 24 hours for measurement of superoxide production using lucigenin-enhanced chemiluminescence at day 10.

* p<0.05 Saline vs DOX

** p<0.05 Saline vs DOX+TRZ and DOX vs DOX+TRZ

# p<0.05 DOX VS NACA+DOX

p<0.05 DOX+TRZ vs NACA+DOX+TRZ and NACA+DOX vs NACA+DOX+TRZ

Figure 12: The average Caspase-3 protein expression at day 10 expressed as a relative ratio in C57Bl/6 mice treated with 0.9% saline (n=7), DOX (n=7), DOX+HER (n=7), NACA+DOX (n=7), NACA+DOX+HER (n=7). Prophylactic NACA administration attenuated the degree of apoptosis in both groups.

* p<0.05 Saline vs DOX

** p<0.05 Saline vs DOX+TRZ and DOX vs DOX+TRZ

# p<0.05 DOX VS NACA+DOX

p<0.05 DOX+TRZ vs NACA+DOX+TRZ and NACA+DOX vs NACA+DOX+TRZ

Figure 13: The average Bax/Bcl-xL ratio expression, at day 10 shown as fold activation in C57Bl/6 mice treated with 0.9% saline (n=7), DOX (n=7), DOX+HER (n=7), NACA+DOX (n=7), NACA+DOX+HER (n=7). Prophylactic NACA administration attenuated the degree of apoptosis in both groups.

* $p<0.05$ Saline vs DOX

** $p<0.05$ Saline vs DOX+TRZ and DOX vs DOX+TRZ

# $p<0.05$ DOX VS NACA+DOX

$p<0.05$ DOX+TRZ vs NACA+DOX+TRZ and NACA+DOX vs NACA+DOX+TRZ

Figure 14: Electron microscopy of representative samples from WT female mouse hearts treated with saline, DOX+TRZ, or NACA+DOX+TRZ at 5800X magnification. Arrows indicate cardiomyocytes displaying myofibril disarray which was most pronounced in DOX+TRZ treated mice.

Figure 15: The amount of fragmented oxidized phospholipids (ng/mg) at 72 hours, in C57Bl/6 female mice treated with 0.9% saline (n=4), DOX (n=3), DOX+HER (n=3), NACA+DOX (n=3), NACA+DOX+HER (n=3). Prophylactic NACA administration attenuated the degree of oxidation in both groups.

Figure 16: RNA analyses in C57Bl/6 female mice at 72 hours post treatment. Treatment groups include Saline (n=3), DOX (n=3), DOX+HER (n=3), NACA+DOX (n=3), and NACA+DOX+HER (n=5). No significant changes were observed between the various treatment arms for any of the markers at 72 hours post treatment.

List of Tables

List of Abbreviations

AC	Adriamycin, Cyclophosphamide
ACEI	Angiotensin-Converting Enzyme Inhibitor
ATP	Adenosine Triphosphate
Bcl-X_L	B-Cell Lymphoma-Extra Large
Bcl-X_S	B-Cell Lymphoma-Extra Small
CHF	Congestive Heart Failure
CMR	Cardiac Magnetic Resonance Imaging
DEX	Dexrazoxane
DNA	Deoxyribonucleic Acid
DOX	Doxorubicin
EF	Ejection Fraction
EGF	Epidermal Growth Factor
EGFR	Epidermal Growth Factor Receptor
EPI	Epirubicin
ErbB (HER) 1/2/3/4	Human Epidermal Growth Factor Receptors 1/2/3/4
FEC	5' Fluorouracil, Epirubicin, Cyclophosphamide
IVS	Interventricular Septum
GSH	Glutathione
LV	Left Ventricle
LVH	Left Ventricular Hypertrophy
LVEF	Left Ventricular Ejection Fraction
LVEDD	Left Ventricular End Diastolic Diameter
LVEDP	Left Ventricular End Diastolic Pressure
LVESD	Left Ventricular End Systolic Diameter
MAPK	Mitogen Activated Protein Kinase
MUGA	Multi-Gated Acquisition Scan
NACA	N-Acetylcysteine Amide
NAD(P)H	Nicotinamide Adenine Dinucleotide Phosphate
NRG	Neuregulin
NYHA	New York Heart Association
PARP	Poly (ADP-ribose) Polymerase
PLAX	Parasternal Long-Axis
PW	Posterior Wall
RAS	Renin-Angiotensin System
ROS	Reactive Oxygen Species
SAX	Short Axis
SR	Strain Rate
TGFα	Transforming Growth Factor Alpha
TnI	Troponin I
Topo II	Topoisomerase II
TRZ	Trastuzumab
TTE	Transthoracic Echocardiogrpahy

TUNEL	Terminal Deoxynucleotidyl Transferase dUTP nick end l labeling
V_{ENDO}	Endocardial Velocity

Chapter 1: Introduction

1.1 Breast Cancer: Statistics, Diagnosis, and Treatment

Breast cancer is the most common cancer among Canadian women and is the second highest cause of cancer related deaths in the country.[2] It is estimated that in 2014, 24,400 women will be diagnosed with breast cancer, accounting for 26% of all new cancer cases in women.[2] Statistics show that 5000 women die from breast cancer annually and that as many as 1 in 9 women will be affected by the disease within their lifetime in Canada.[2]

Advancements since the 1980's in the screening and treatment for high risk cancer patients has decreased breast cancer related deaths in all age groups.[2] The decreased rates of morbidity and mortality in the past few decades can be attributed to the development of novel imaging techniques, which allow for the early detection of tumors.[3-6] The current combination of imaging modalities used in breast cancer screening include full-field digital mammography, magnetic resonance imaging, ultrasonography, and positron-emission tomography.[4, 5, 7] Although the physical exam is a routine apart of the preliminary screening procedure, it is often combined with an imaging technique in order to detect tumors that are smaller and at a significantly earlier stage.[4] Furthermore, the combination of novel targeted therapies and genetic screening protocols for individuals with familial history of breast cancer have also contributed to decreasing the mortality and morbidity associated with this disease.[8]

Breast cancer treatment is multifaceted, most commonly comprised of surgery, radiation therapy, chemotherapy including anthracyclines, and the recent addition of monoclonal antibodies. Surgical approaches vary depending on location and size of affected nodes. Surgical resection can range from node specific lymphadenectomies to complete radial mastectomy, which includes the complete removal of breast tissue.[7] The use of radiation therapy, in conjunction with surgical and chemotherapeutic treatments, has proven to be very beneficial in early breast cancer treatment.[9] Adjuvant radiation therapy has been shown to reduce the risk of local recurrence (18% chemotherapy alone, 7% combination therapy, $p=0.002$[10] when used in addition to chemotherapy).[10] The mainstay of the chemotherapeutic regimen for breast cancer therapy includes the combination of 5-fluorouracil-epirubicin-cyclophosphamide (FEC).[2] Recent advancements have incorporated the use of monoclonal antibodies in patients who express estrogen or progesterone receptors.[11]

1.2 Breast Cancer Therapy and Cardiac Damage

Many survivors of breast cancer who undergo therapy with anthracycline therapy followed by monoclonal antibodies often have substantial morbidity and mortality due to the delayed chemotherapy induced cardiac disease. Given this, there is a need for an effective protective regimen, which could attenuate the drug induced cardiac dysfunction associated with breast cancer therapy. Recent efforts have been directed to discovering the underlying mechanisms responsible for the cardiotoxic side effects of breast cancer treatment. Many studies have revealed that an increase in oxidative stress, due to the production

of chemotherapy-induced free radicals, plays a pivotal role in damaging cardiomyocytes.[12-14]

Given this proposed mechanism of damage, recent efforts to attenuate chemotherapy induced cardiac dysfunction have led to investigations into the use of prophylactic antioxidant treatment. N-acetylcysteine (NAC) is an antioxidant which was seen to significantly reduce free radical induced damage in cardiomyocytes *in vitro*, but proved to be ineffective *in vivo*.[15] The ineffectiveness of NAC has been attributed to its low bioavailability and its inability to cross the lipid bilayer of cells due to its polarity. The novel antioxidant N-acetylcysteine amide (NACA), which is a structural analog to NAC offers an increased lipophilicity making it much more bioavailable. Investigating the use of NACA as a protective agent in the prevention of chemotherapy induced cardiotoxicty is warranted.

Chapter 2: Literature Review

2.1 Anthracycline History

Anthracyclines have been used as antibiotics since the late 1930s.[16] Further characterization of the chemical properties of anthracyclines during the 1960s led to the discovery of their potential anti-tumor properties.[16] Isolations from the pigment producing soil bacterium, *Streptomyces peucetius varcaesitue,* lead to the creation of two anthracycline drugs, known as Daunorubicin (DNR) and Doxorubicin (DOX).[16, 17] Both of these drugs have been extensively characterized due to their wide range anti-tumor properties against human cancers.[17, 18]

Doxorubicin and Daunorubicin are very similar in chemical structure. The two drugs differ by a single termination chain in which Doxorubicin terminates with a primary alcohol while Daunorubicin terminates with a methyl group.[19, 20] This small difference in structure has significant consequences for both of these drugs. The structure of Doxorubicin causes it to be highly lipophilic allowing it to effectively penetrate the cellular lipid bilayer, thus increasing its half-life within the human body (Figure 1). [21] Both of these drugs have been used to combat various cancers, with Doxorubicin being one of the key components for breast cancer treatment. The clinical use of Doxorubicin has also been extended to childhood solid tumors, soft tissue sarcomas, and lymphomas. [16, 22, 23]

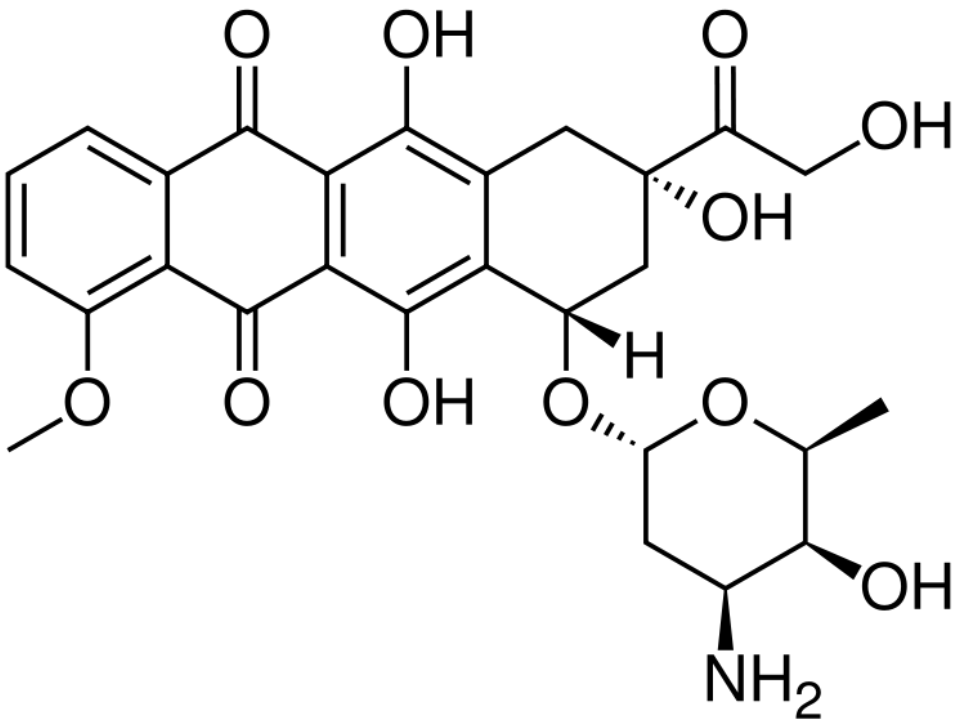

Figure 1: The chemical structure of Doxorubicin (8S,10S)-10-{[(2R,4S,5S,6S)-4-amino-5-hydroxy-6-methyloxan-2-yl]oxy}-6,8,11-trihydroxy-8-(2-hydroxyacetyl)-1-methoxy-5,7,8,9,10,12-hexahdrotetracene-5,12-dione.

2.2 Anthracyclines: Doxorubicin Anti-Cancer Mechanisms

Doxorubicin (Adriamycin) has been reported to reduce solid tumor size by multiple different mechanisms of action. The anti-tumor activity of Doxorubicin involves the drug's ability to intercalate between base pairs of DNA, thus inhibiting the rapidly dividing tumor cells from replicating and prolferating.[20] Recent studies have discovered a novel anti-tumor mechanism, which involves histone eviction from chromatin of rapidly dividing tumor cells.[24] Histone eviction deregulates the transcriptome (mRNA, tRNA, and rRNA) in cancer cells and can induce apoptosis and reduce tumor size.[24] Other modes of action for

Doxorubicin include: DNA crosslinking, interference with DNA unwinding, direct membrane damage, and altered DNA binding and alkylation. [22, 25, 26] The two most widely accepted and characterized modes of anthracycline function are the inhibitory action on the enzyme topoisomerase II and free radical generation.[20, 21, 26]

Topoisomerase II (topo-II) is an enzyme that changes the topological state of DNA by introducing or removing DNA supercoils, which has direct implications on DNA replication and transcription.[27] The enzymes' direct effect on DNA, and ultimately cell proliferation, has made it a popular target for anti-tumor therapy.[27] Doxorubicin is a therapeutic agent that is a cleavable complex-forming topoisomerase II inhibitor that has been used to treat cancer since 1963.[28, 29] Doxorubicin acts by inhibiting mammalian cell DNA and RNA synthesis, thus effectively arresting uncontrolled tumor growth. [20] Specifically, topo-II, under normal physiological conditions functions by cleaving the DNA double helix and allowing the passage of DNA fragments through the break before re-joining the two strands.[27] This is essential during normal DNA unwinding, as the process introduces supercoils into the DNA resulting in the inability to further unwind.[27] Through the enzymatic function of topo-II, the DNA double helix is cleaved, thereby allowing the supercoiled segments to pass through the break before rejoining of the two strands, allowing the DNA to relax and continue to unwind.[27, 30] Doxorubicin effectively inhibits this enzyme's function by creating stable DNA-topo II complexes that prevent re-annealing and leave DNA lesions within the unwinding strand, eventually resulting in programmed cell death.[29]

In contrast to the protein associated DNA strand breaking of topo-II, the second most widely accepted anti-tumor function of anthracylines involves DNA strand breaks associated with production of reactive oxygen species.[22] The mechanism of DOX induced generation of superoxides involves the quinone structure of DOX, which allows it to act as an electron acceptor in redox reactions. Once DOX accepts an electron, it produces a semi-quinone free radical.[23, 25] In an aerobic environment, this unstable semi-quinone readily donates its unpaired electron to molecular oxygen generating a superoxide radical.[25] When these superoxides come into contact with DNA, they lead to severe damage by causing partial or complete DNA strand breaks. In addition, DOX can also complex with iron and form intermediates that are capable of binding DNA and producing partially reduced forms of oxygen.[23] DOX has also been shown to reduce the levels of a free radical scavenging protein known as glutathione (GSH) peroxidase.[31] The multiple anti-tumor properties of DOX solidify its efficacy as an anti-cancer agent.

2.3 Anthracyclines: Doxorubicin-induced Cardiotoxicity

Doxorubicin has become the most potent, and widely used broad-spectrum anti-tumor agent since its introduction in the mid 1960's.[31] Through the extensive use of this drug, it has become evident that DOX is highly effective in the cancer setting, but its clinical use has been limited due to its associated adverse side effects.[31] Side effects associated with DOX include myelosupression, nausea, vomiting, cardiac arrhythmia, and cardiac dysfunction.[19] The most limiting side effect of DOX is the inherent cardiotoxicity associated with the drug,

which leads to advanced congestive heart failure (CHF). This drug-induced cardiomyopathy is non-reversible and presents itself in a dose-dependent fashion, thus limiting the clinical use of DOX.[21] Many studies have reported that a lifetime cumulative dosage of over 500mg/m^2 of body surface area places individuals receiving DOX therapy at a high risk for drug-induced cardiac dysfunction. [19, 21, 32] Studies have shown that patients who receive 500-550 mg/m^2 of DOX go on to develop CHF in 4% of cases. The incidence of CHF increased to as much as 18% in patients receiving between 550-600 mg/m^2, and has been reported as high as 36% in patients receiving over 600 mg/m^2. [19, 33] Other compounding risk factors for DOX mediated cardiotoxicity include age greater than 70 years, left chest radiotherapy, and a history of hypertension. [19, 34] Given the severity of the cardiotoxicity associated with DOX treatment, risk stratification of patients receiving the therapy remains the most important factor in the prevention of DOX mediated cardiac dysfunction. Finding an equilibrium between anti-tumor effectiveness while maintaining the lowest degree of cardiotoxicity remains an ongoing challenge.

2.4 Monoclonal Antibodies: The Human Epidermal Growth Factor Receptor

Human epidermal growth factor receptors (ErbB) are a group of tyrosine kinases (RTK) that comprise a family of receptors responsible for mediating cell growth, differentiation, and survival. [35] This family of RTK's consists of four closely related receptors: HER-1, HER-2, HER-3, and HER-4, all of which participate in cellular cross talk formulating an intricate cellular signaling network. [35, 36] Each of these RTK's is defined as a cell surface receptor that is

composed of 3 distinct domains; (i) a single membrane-spanning domain; (ii) a ligand activated tyrosine kinase domain; and (iii) a carboxy-terminal regulatory domain. [37, 38]

The activation of the ErbB receptor pathways begins with a specific ligand-receptor interaction that takes place on the extracellular domain of the receptor. The numerous ligands that bind the receptor family are very specific in which receptor isoform they interact with. Ligands that are specific to HER-1 include epidermal growth factor (EGF), transforming growth factor (TGF-α), and amphiregulin. Some ligands do not discriminate between pairs of receptors due to the homology between their various domains. Ligands that bind to HER-3 and HER-4 include *neu*-differentiating factor (NDF), neuregulins (NRG), and heregulins. In addition, there are also some ligands that specifically bind the HER-1 and HER-4 isoforms. These ligands include betacellum, epiregulin, and heparin-binding EGF-like growth factor. [38, 39] There have been no identified ligands that directly bind the HER-2 isoform. HER-2 is known to participate in heterodimerization with all of the other HER isoforms, thus acting as a common receptor for all other isoforms. [40, 41]

The HER-2 isoform has been known to be specifically important in the breast cancer setting. Upon stimulation by a ligand including cytokine interleukin (IL)-6 or NRG, the receptor dimerizes with adjacent HER receptor isoforms. Upon dimerization, cell proliferation and survival pathways are initiated through Ras-Raf-MAPK and PI3K/Akt respectively (Figure 2). [37] Overexpression of the HER-2 receptor directly affects crosstalk between adjacent receptors and other

signaling pathways that are responsible for cell proliferation and apoptotic resistance, thereby leading to an uncontrolled proliferation. [36]

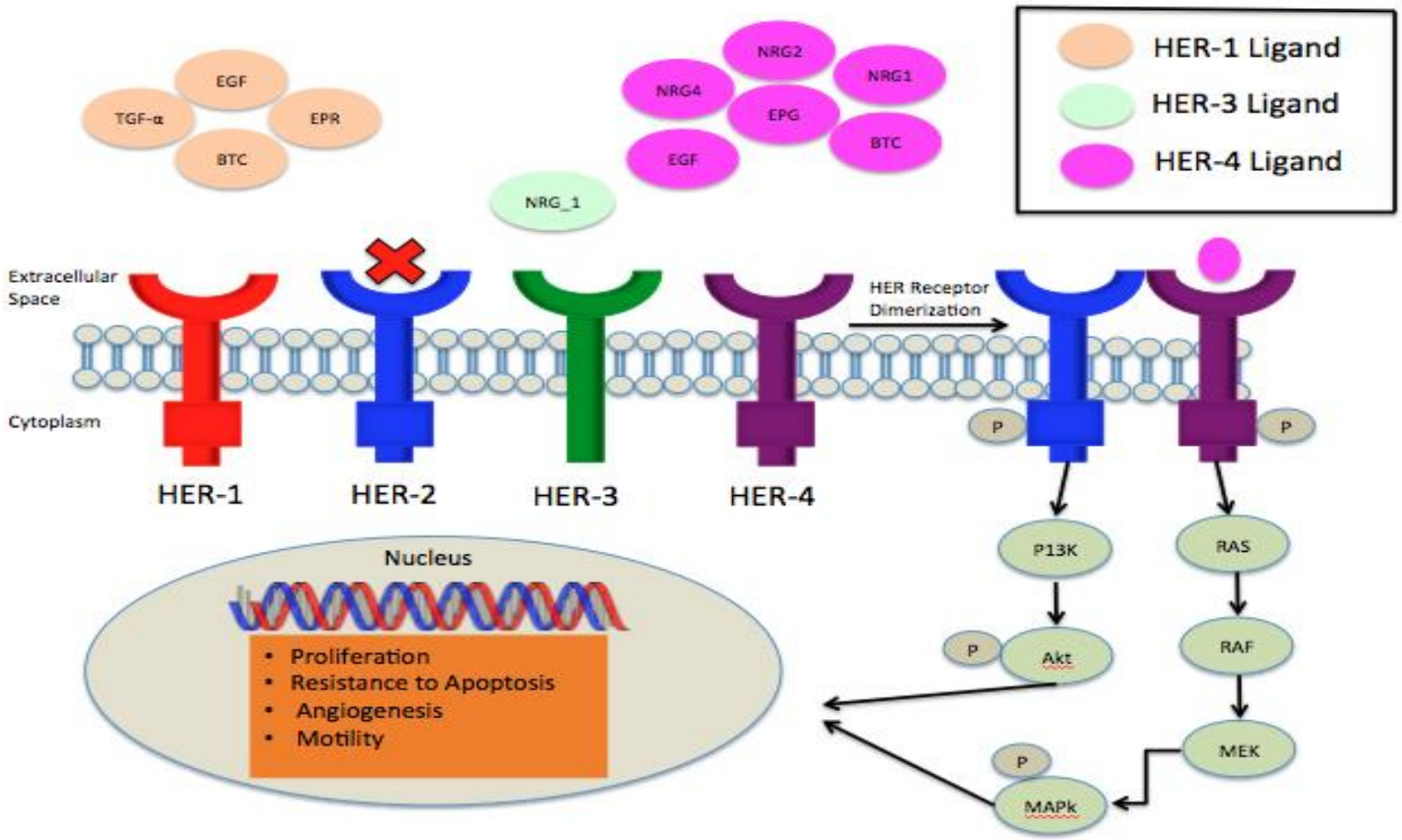

Figure 2: Heterodimerization of the human epidermal growth factor receptor 2 (HER-2) with adjacent receptors (HER-1, HER-3, HER-4) leads to the downstream activation of the P13K and Ras-Raf-MAPK pathways, which lead to increased cell proliferation, motility, apoptotic resistance, and angiogenesis. [1]

2.5 Monoclonal Antibodies: Breast Cancer and Overexpression of HER-2

The overexpression of human epidermal growth factor receptors is known to be intimately involved in a multitude of cancers. [42] It has been reported that as many as 30% of breast cancer patients present with HER-2 overexpression. Certain breast cancers, such as ductal carcinoma, are known to overexpress HER-2 in 90% of cases.[43] Overexpression of HER-2 is associated with a significantly more aggressive tumor phenotype and an increased mortality rate.[43] Breast tissue that is positive for HER-2 overexpression is associated with gene amplification for the HER-2 receptor gene. This overexpression leads to an increased number of cell surface receptors, which effectively increases the rate of cell division leading to proliferation, causing aggressive tumor growth.[44, 45]

The overexpression of HER-2 occurs very early in the progression of breast cancer making its early detection crucial to patient outcomes. This early detection is often achieved through immunohistochemistry (IHC), chromogenic *in situ* hybridization (CISH), and silver enhanced *in situ* hybridization (SISH).[46] In Canada, the guidelines most often employ the use of FISH and IHC for the detection of HER-2 overexpression. The utility of IHC for this detection uses monoclonal antibodies that recognize and interact with HER-2 in biopsy tissue sections taken from the patient, in order to stratify patients into HER-2 positive or negative groups. [47, 48]

2.6 Monoclonal Antibodies: Trastuzumab and the Inhibition of HER-2

Trastuzumab (TRZ) (Herceptin, Genetech Inc.) is currently used for the treatment of breast cancer patients who are positive HER-2 overexpression.[43] This monoclonal antibody is directed against the extracellular domain of HER-2 and acts by binding to this domain, ultimately preventing the dimerization of HER-2 with adjacent human epidermal growth factor receptors.[49] Interruption of the HER-2 dimerization effectively disrupts downstream cell survival and proliferation pathways including Ras-Raf-MAPK and PI3K/Akt.[36] In addition to the anti-dimerization properties of TRZ, the monoclonal antibody also down-regulates the accumulation of the HER-2 receptor by enhancing its internalization and degradation.[50] The mechanism of action of TRZ involves two proteins, $P27^{Kip1}$ and the Rb-related protein p130. Both of these proteins are up-regulated upon TRZ treatment, which causes a significant decrease in the number of cells entering the S-phase of the cell cycle.[51] It has also been postulated that the interaction between TRZ and the human immune system, via its immunoglobulin G1 Fc domain, may potentiate the anti-tumor effects of this monoclonal antibody. [51]

2.7 Monoclonal Antibodies: The Clinical Use of Trastuzumab

Following treatment with an anthracycline based chemotherapy regimen, women who overexpress HER-2 are treated with TRZ in the adjuvant setting of breast cancer.[43, 49, 52] The dosage of TRZ treatment begins with a loading phase in which patients are administered 8 mg/kg, followed by weekly dosages of 6 mg/kg for a total of one year, when administered as singular therapy.[53] If the

breast cancer has metastasized to other organ systems, treatment with TRZ includes a loading dosage of 4 mg/kg followed by maintenance doses of 2 mg/kg administered every 3 weeks.[54] Studies have validated TRZ as a front-line treatment option when used in combination with chemotherapeutic agents such as paclitaxel, or anthracycline/cyclophosphamide therapies.[52, 55] It has also been reported that when TRZ is used in conjunction with anthracycline based therapy, the combination therapy can reduce cancer related death by approximately 33%.[49, 52, 53, 56, 57]

There have been four major multi-center randomized control studies that have evaluated the efficacy of TRZ in the adjuvant setting of breast cancer. These studies include the Herceptin Adjuvant Trial [58], National Surgical Adjuvant Breast and Bowel Project Trial B-31 (NSABP), North Central Cancer Treatment Group Trial N9831 (NCCTG-N-9831), and the Breast Cancer International Research Group 006 Data Trial (BCIRG 006)[53, 56, 59, 60] These trials solidified the efficacy of TRZ use following anthracycline treatment. The main findings of these studies include an overall reduction in recurrence of malignancies by 50%, and mortality by 33%, in women who received adjuvant treatment with TRZ. Due to the positive results of these impactful trials, TRZ treatment has become an essential component in anthracycline-based chemotherapy for breast cancer.

Clinical trials have also evaluated the use of TRZ in conjunction with standard chemotherapy in the 10% of women suffering from breast cancer who present with metastatic malignancies.[52] Of the 10% of women with metastatic malignancies, 35-45% of patients present with overexpression of HER-2.[52]

Women who received chemotherapy with the addition of TRZ in the metastatic setting of breast cancer experienced a 20% mortality risk reduction. Despite the beneficial anti-cancer properties of TRZ, its cardiotoxic side effects cannot be ignored. Approximately 27% of women receiving the combination therapy went on to suffer cardiac dysfunction, while only 8% of women receiving standard chemotherapy alone faced these side effects.[52]

2.8 Monoclonal Antibodies: Trastuzumab Induced Cardiomyopathy

The anti-cancer benefits of Trastuzumab have made the monoclonal antibody a mainstay in the treatment of breast cancer in women. Despite its therapeutic benefits, the risk of developing a drug-induced cardiomyopathy is a major concern. This drug-induced cardiotoxicity is significantly potentiated when TRZ is administered following standard anthracycline based therapy. The Cardiac Review and Evaluation Committee has outlined four general criteria to diagnose TRZ related cardiac dysfunction. The criteria include: congestive heart failure (CHF) symptoms; symptoms associated with CHF including a S3 gallop and tachycardia; a 5% or greater decrease in left ventricular ejection fraction (LVEF) with CHF symptoms; or finally, a 10% decline in LVEF without CHF symptoms.[61] Positive diagnosis for TRZ related cardiac dysfunction includes any one of the four mentioned criteria.

In the clinical setting, the adverse side effects of adjuvant TRZ therapy include the development of class I-IV CHF as outlined by the New York Heart Association (NYHA). The NYHA classification of CHF ranges from class I which is defined as mild CHF with no limitation in physical activity, to class IV which is

defined as severe shortness of breath at rest, with an inability to carry out physical activity without discomfort.[62] The four clinical trials that evaluated the development of LV systolic dysfunction in adjuvant TRZ therapy showed that approximately 5-10% of patients developed cardiac dysfunction. The HERA trial demonstrated that the incidence of symptomatic heart failure in women receiving TRZ was below 1% while the Trial B-31 showed that it was 4.1%.[52] The results from the N9831 placed the percentage of patients who underwent TRZ therapy and developed CHF to be at 3%. Given the results form these studies, the incidence of symptomatic heart failure from breast cancer patients treated with TRZ lies between 1-4%.

In addition to these trials, our group evaluated 152 HER-2 positive breast cancer patients who underwent adjuvant therapy with TRZ. The objective of this study was to retrospectively evaluate the incidence of cardiac dysfunction, and to identify the reversibility in the HER-2 positive breast cancer population receiving TRZ in adjuvant therapy.[63] Out of the 152 women, 24% developed TRZ mediated cardiomyopathy, the majority of whom were asymptomatic.[63] The study went on to describe cardiac risk factors that predisposed patients to developing TRZ related heart dysfunction. Factors that contributed to development of cardiomyopathy included preexisting hypertension, smoking, and a family history of premature coronary artery disease. This study was unique due to the fact that although past clinical trials have shown the incidence of TRZ -mediated cardiomyopathy to be less than 10%, this real world study places this risk as high as 25%.[63]

The prevalence of TRZ mediated cardiotoxicity is highest in the treatment of metastatic breast cancer. This is primarily attributed to the fact that TRZ is administered in conjunction with an anthracycline based therapy in the metastatic setting of breast cancer. Studies have demonstrated that 27% of women receiving treatment with TRZ along side standard anthracycline therapy go on to develop NYHA class III or IV heart failure.[44] This aggressive treatment approach has become common practice in this subset of patients who have poor prognosis with mean a life expectancy of 9 to 12 months. The treatment regimen is often palliative with the use of mitotic inhibitors, such as paclitaxel following TRZ therapy. With the limited treatment options available for metastatic breast cancer, aggressive therapy with an increased risk of cardiotoxicity has become the accepted method of treatment.[64]

2.9 Mechanism of Trastuzumab-Induced Cardiac Dysfunction

The pathogenesis of TRZ induced cardiotoxicity includes three main mechanisms. One of these mechanisms includes the induction of cell death pathways through the alteration of anti- and pro- apoptotic proteins. Many pathological molecular insults may initiate the genetically programmed cell death pathway known as apoptosis. Specifically, the expanding family of proteins known as the Bcl-2 family contains both pro-apoptotic and anti-apoptotic elements.[65] The ratio between these two subsets of proteins is a determinant of whether a cell will initiate apoptosis, or strive as a healthy living cell. It has been postulated that once TRZ binds the HER-2 receptor, there is an immediate decrease of the anti-apoptotic protein Bcl-X_L, as well as an increase in the pro-

apoptotic protein Bcl-X_S.[66] These apoptotic proteins play a critical role in mitochondrial function, thus making the altered ratio of these proteins beneficial towards fighting cancer but detrimental to cardiac health. The increase in pro-apoptotic Bcl-X_S causes mitochondrial dysfunction and initiates cell death in cardiomyocytes.[66, 67]

The second proposed mechanism for TRZ induced cardiac damage is via increased stimulation of the renin-angiotensin system. The inhibition of cell survival pathways caused by the binding of TRZ to the HER-2 receptor is known to stress the myocardium. This increased stress causes a significantly increased level of circulating angiotensin II (ANG II). Increased ANG II causes a decrease in NRG-1 protein levels, ultimately reducing the amount of a key regulator in cell survival signaling pathways.[68] In addition, ANG II also inhibits the already reduced amount of NRG-1 from binding to the HER-4 receptor, thus severely reducing the activation of cell survival pathways.[68] Finally, ANG II also binds to the angiotensin 1 receptor, which activates a cascade resulting in the production of reactive oxygen species (ROS). The activation of this cyclic superoxide production causes increased oxidative stress (OS), which negatively impacts cardiomyocytes, thus potentiating the drug-induced cardiotoxicity associated with TRZ.[69]

Finally, the third mode of action for TRZ induced cardiac dysfunction stems from the anti-dimerization properties of TRZ. By inhibiting the ability for HER-2 to dimerize with the other HER family receptors, downstream cell survival pathway signaling is significantly reduced, ultimately causing decreased

resilience of cardiomyocytes. The inability to deal with excess stress places active cardiomycoytes at risk of apoptosis through increased OS.[70, 71] Active cardiomyocytes have high metabolic demands for adenosine triphosphate (ATP), which is produced by the mitochondria. Increased metabolic demand leads to the generation of ROS through ATP production via the electron transport chain in the mitochondria. This increased ROS within the cardiomyocyte leads to development of cardiac dysfunction, potentially through the initiation of apoptotic cell death pathways.[67, 72]

2.10 Oxidative Stress: Activated Oxygen Species

Activated oxygen species include singlet oxygen molecules, superoxide radicals, and hydroxide radicals that are produced by the incomplete reduction of oxygen.[73] These reactive oxygen species are detrimental to surrounding tissue due to their short half-lives, unstable nature, and highly reactive state.[74] They are able to react with unsaturated lipids causing a chain reaction that results in lipid peroxidation.[73] These free radicals are also known to oxidize of sulphydryl groups in proteins as well as damage DNA strands.[75] Furthermore, increases in OS have also been shown to cause auto-oxidation of catecholamines, causing cardiac dysfunction.[73] Ischemia-reperfusion studies have also shown that increases in ROS can interfere with calcium transport in the sarcoplasmic reticulum resulting in abnormal cardiomyocyte function.[73] Ultimately, increases in ROS can have devastating effects on the normal physiology of cells and organ systems from a multitude of pathways. Increased awareness of this potential

damage has lead to the investigation of the effects of increased ROS caused by chemotherapeutic regimens for various malignancies.

2.11 Oxidative Stress (OS): A Product of Breast Cancer Therapy

OS is defined as an imbalance between the systemic manifestation of reactive oxygen species, and a biological systems ability to detoxify the reactive intermediates. Chemotherapy for breast cancer has been known to cause cardiac dysfunction primarily through an increase in OS. Anthracycline based therapy is known to influence two specific signaling pathways: mitogen-activated protein kinases (MAPKs) and the transforming growth factor-beta 1 (TGF-β1)/SMAD cascade.[73]

The increase in OS through breast cancer therapy has a significant impact on the mitogen-activated protein kinases (MAPK). The MAPK pathway is responsible for relaying information from the cell surface all the way to the DNA in the nucleus of cells. This pathway is intimately involved in regulating cell functions including proliferation, differentiation, mitosis, and apoptosis.[76] Through both JNK and P38 pathways, the expression of key apoptotic proteins including Bax, Caspase, and PARP is up-regulated, while expression of anti-apoptotic proteins including Bcl-2, and Bcl-X_L are down-regulated.[77] Moreover, anthracycline induced OS also down-regulates AKT, which is a serine/threonine kinase that promotes cell survival in cardiomyocytes.[77] AKT is normally involved in protecting cells from apoptosis by phosphorylating substrates that directly down-regulate apoptotic machinery.[78] The effects of OS on the MAPK pathway

and the ensuing apoptosis of cardiomyocytes significantly impacts the clinical use of anthracycline based treatment regimens for breast cancer patients.

DOX related increases in OS also up-regulates the Transforming Growth Factor-β1/SMAD cascade. The TGF-β1 pathway is involved in many cellular processes in adult organisms. This pathway is responsible for cell growth, differentiation, apoptosis, and homeostasis. The TGF-β1 pathway functions by a series of phosphorylation events, which eventually activate the receptor regulated SMADs, which then complex with other SMAD proteins.[79] These SMAD complexes localize in the nucleus of the cell where they function as transcription factors allowing them to regulate gene expression.[79] The increased activity in the TGF-β1 pathway causes proliferation of fibroblasts, increased synthesis of collagen, and augmented expression of extracellular matrix proteins.[80] The intricate relationship between the SMAD and the TGF-β1 pathways, once up-regulated, causes unwanted cardiac fibrosis with subsequent adverse cardiovascular remodeling, eventually resulting in DOX mediated cardiomyopathy.[81, 82]

In addition, DOX+TRZ induced OS has also been reported to damage the cardiac cytoarchitecture. DOX is known to decrease the function of GATA-4 and increase calpain, ultimately causing a loss of both myofibrillar and sarcolemmal integrity (Figure 3). GATA-4 is a transcription factor from the zinc finger family that is essential in the expression of sarcomeric protein.[83] The products of GATA-4 regulated genes includes the alpha myosin heavy chain (α-MHC) and troponin I (cTnI), both of which are essential for normal cardiomyocyte function.[84, 85]

Recent studies have shown that the preservation of GATA-4 can attenuate DOX induced cell death, thereby displaying the importance of this key molecular entity.[86, 87] Moreover, DOX is known to cause intracellular calcium overload leading to the activation of calcium dependent proteases known as calpains.[88, 89] Calpains are responsible for cleaving cytoskeletal as well as myofilmental proteins including αMHC, cTnI, desmin and dystrophin, ultimately causing loss of cardiomyocyte integrity and function (Figure 3).[90, 91] A recent study has shown that DOX administration increased calpain activity in cardiomyocytes and promoted cell death.[92]

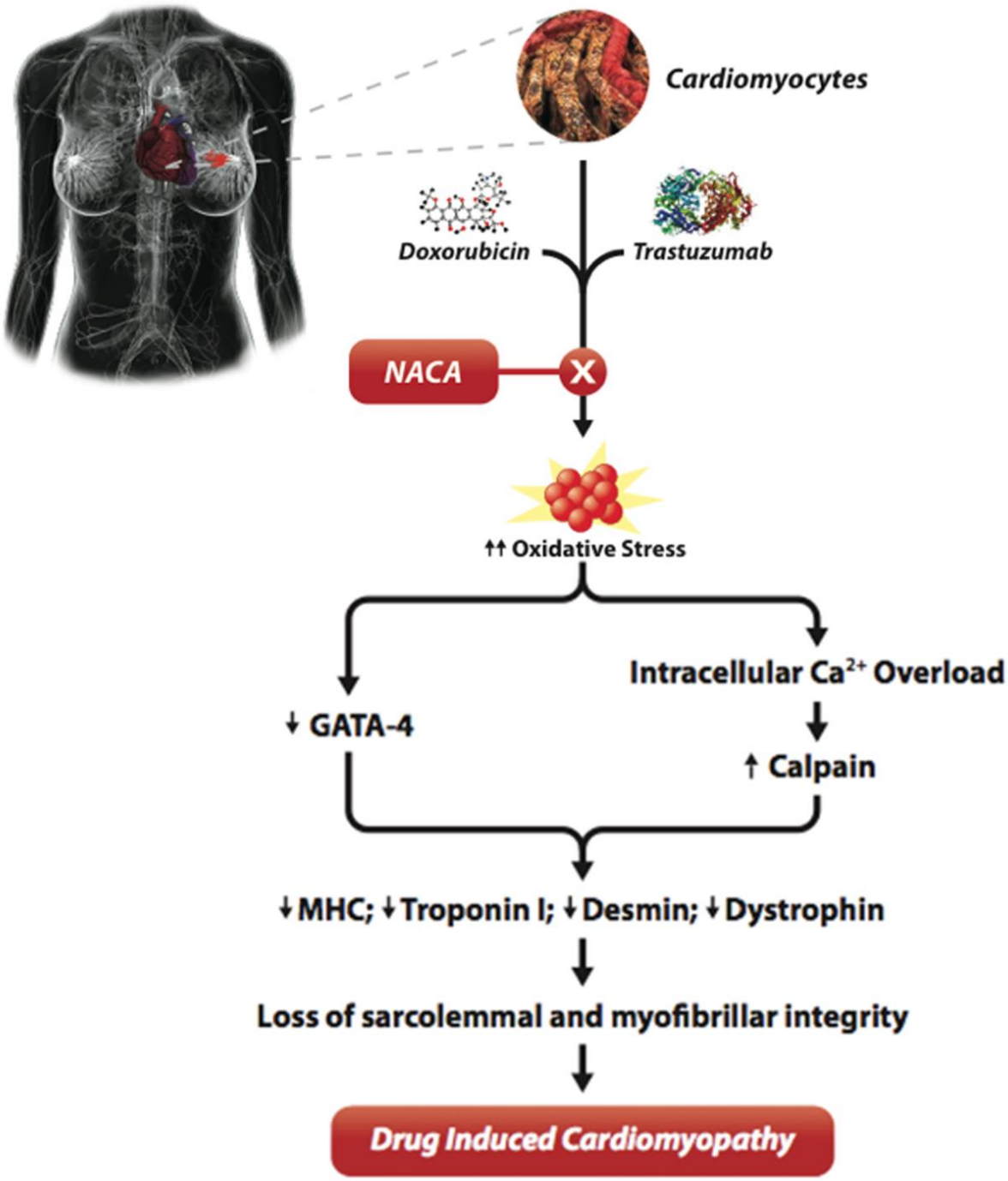

Figure 3: A schematic diagram illustrating the proposed roles of N-acetylcysteine amide (NACA), oxidative stress (OS), GATA-4, calpain, and myofibrillar/cytoskeletal proteins in Doxorubicin + Trastuzumab mediated cardiotoxicity.

Given the inherent increases in OS that are associated with breast cancer therapy, recent efforts have shifted towards potentially preventing the detrimental effects associated with chemotherapeutic regimens. The prophylactic use of novel anti-oxidants in the prevention of chemotherapy induced cardiac dysfunction has gained recent attention.

2.12 OS: Cellular Antioxidants

Cellular antioxidant defenses include two classes of compounds, enzymatic antioxidants and non-enzymatic antioxidants. Superoxide dismutase, catalase, and glutathione peroxidase are enzymatic defenders against OS, which are readily found in cells.[93] Cells also contain defensive species that are not enzymatic in nature, but instead exert their protective effects through their unique organic structure. The common non-enzymatic antioxidants include tocopherols, carotenoids, retinol, melatonin, ubiquinol, ascorbic acid, and most importantly, glutathione (GSH). [94] The structure of all of these non-enzymatic antioxidants allows them to quench potentially damaging oxidative species before they exert their effect on cellular components. Through this process, the antioxidant species is able to consume free radicals, which in turn transforms the antioxidant to a far less reactive product, or a completely inert species.[95]

Glutathione is a very important antioxidant species that provides protection to cells from the negative effects of OS. The tripeptide contains a glycine, cysteine, and glutamic acid in its protein backbone, allowing it to serve as a key mediator of homeostasis in cells. [96] The GSH peroxidase system is known to be a critical defense mechanism against activated oxygen species.[97] During GSH

peroxidase mediated protection, GSH is reduced to GSSG by accepting the free radical from the reactive oxygen species.[97] The maintenance of the GSH reservoir is essential to maintain cellular viability, and adequate protection from OS. The maintenance of the GSH pool has also shown to be very important in chemotherapy related increase in OS. In addition to GSH, there has been an effort to explore the benefits of pharmaceutical agents, which may also offer protection from the negative effects of activated oxygen species by either maintaining the levels of GSH, or acting as free radical electron acceptors themselves.

2.13 Prevention of Chemotherapy Induced Cardiac Dysfunction: NAC

N-acetylcysteine (NAC) is a pharmaceutical drug that is a derivative of cysteine, which contains an acetyl group attached to a nitrogen atom. The clinical use of NAC includes treatment for acetaminophen toxicity, mucolytic therapy, and as a nephron-protective agent against radio-contrast induced nephropathy.[98-100] The protective effects of NAC are rooted in its structure, which contains L-cysteine, a precursor to the biological antioxidant GSH (Figure 4). Administration of NAC is able to replenish the GSH reservoir, effectively allowing cells to dissipate an increase in OS.[101]

The clinical use of NAC as a cardioprotective agent has been evaluated in DOX mediated cardiac dysfunction.[15] NAC has failed to show any beneficial properties in DOX mediated cardiac dysfunction.[15, 102] A small clinical trial of 20 patients randomized to either placebo, or prophylactic administration of NAC (140mg/kg) one hour before a single intravenous (IV) injection of DOX evaluated the drugs cardioprotective potential. Endomyocardial biopsies were

performed at baseline, 4-hours post drug administration, and 24-hours post drug administration. The three time points of both placebo and NAC groups showed no significant differences with respect to cardiomyocyte injury. Both groups developed tubular necrosis and mitochondrial swelling, suggesting that NAC was unable to serve as a cardioprotective agent in DOX-induced cardiomyopathy.[15]

In addition to the inability to validate NAC as a cardioprotective agent, the drug also has a number of adverse side effects. NAC is known to be a pro-oxidant, a suppressant to respiratory bursts, and a toxic agent causing ammonia accumulation in patients with pre-existing liver dysfunction.[103] Furthermore, NAC also contains a negatively charged carboxyl group at physiological pH, which significantly lowers its bioavailability thus limiting it from becoming a suitable cardioprotective agent in the clinical setting (Figure 4).

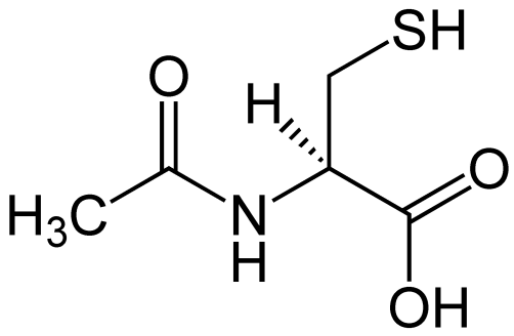

Figure 4: The chemical structure of NAC (2*R*)-2-acetamido-3-sulfanylpropanoic acid[103]

2.14 Prevention of Chemotherapy Induced Cardiac Dysfunction: NACA

Recent efforts to prevent chemotherapy induced cardiac dysfunction have lead to the creation of a thiol structural analog of NAC known as N-acetylcysteine amide (NACA). The chemical structure of NACA contains an amide in place of the carboxyl group that is found in NAC. This chemical manipulation significantly increases the bioavailability of NACA by allowing it to traverse the cellular lipid bilayer.[104, 105] The anti-oxidant properties of NACA are rooted in its chemical structure, mirroring the same mechanism of action as its structural counterpart, NAC (Figure 6). NACA is able to maintain the intracellular levels of GSH in cells in order to reduce the effects of OS in a multitude of tissues. This is accomplished through the ability of NACA to transfer its thiol group to oxidized glutathione (GSSG), thus regenerating GSH through redox chemistry.[105] The increased potency and bioavailability of NACA allows it to be administered at much lower dosages, thereby significantly decreasing the adverse effects that have been seen in NAC toxicity. There have been no reports of adverse effects of NACA in literature to date.[104-107]

Investigations into the anti-oxidant properties of NACA have demonstrated that the compound is able to scavenge free radicals, and protect red blood cells from OS through the prevention of ROS-induced activation of JNK, MAPK pathways, and matrix metalloproteinases.[105, 106] In addition, another study exploring the anti-oxidant properties of NACA demonstrated that NACA (250mg/kg) was able to protect the blood brain barrier from OS in mice exposed to methamphetamine.[104] Studies have also been conducted in an *in*

vitro model using embryonic rat cardiomyocytes exposed to DOX. The parameters of the study included DOX induced increases in ROS, decrease in anti-oxidant levels, and lipid peroxidation.[107] The studies main findings indicated that NACA was able to reduce the levels of OS as well as lipid peroxidation, while increasing the levels of GSH and the GSH/GSSG ratio.[107] The data from these studies provides a strong rationale to investigate whether or not NACA may provide cardioprotection in DOX+TRZ mediated cardiac dysfunction in the *in vivo* setting.

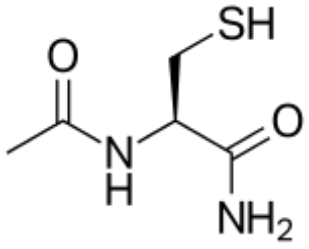

Figure 5. The chemical structure of NACA (2*R*)-2-Acetamido-3-sulfanylpropanamide[108]

Chapter 3: Rationale, Hypothesis, and Aims

3.1 Rationale:

It is clear from the literature review presented that breast cancer rates are on the rise. The clinical use of high dose anthracycline and Trastuzumab based therapy has become the mainstay of disease treatment. The inherent cardiotoxicity related to use of the anti-cancer drugs DOX and TRZ is still a major public health concern. The oxidative stress pathway is intricately involved in the pathogenesis of this drug induced cardiotoxicity, and we still have to devise ways and means to successfully interfere with this pathway. The study has two main aims to address this problem, including:

3.2 Aims and Hypothesis:

Aim 1: To investigate whether DOX+TRZ mediated OS leads to disruption of myofibrillar and sarcolemmal integrity in an acute *in vivo* female mouse model of chemotherapy induced cardiac dysfunction.

Hypothesis: DOX+TRZ treatment will cause myofibrillar and sarcolemmal disruption leading to cardiomyocyte damage. Furthermore, we hypothesize that this loss of cytoskeletal and myofibrilliar integrity will be due to increases in OS. Specifically, we will focus on the degree of left ventricular (LV) systolic dysfunction, histological damage, lipid peroxidation, and degree of apoptosis in wild type C57Bl/6 mice treated with DOX, TRZ, or the combination of DOX+TRZ.

Aim 2: To investigate whether the prophylactic administration of the antioxidant NACA will be cardioprotective by preventing some or all of the

changes in myofibrillar and cytoskeletal proteins in an acute *in vivo* female mouse model of chemotherapy induced cardiac dysfunction.

Hypothesis: NACA will attenuate DOX+TRZ mediated cell death. We hypothesize that as compared to WT controls, female mice receiving prophylactic administration of NACA will have elevated levels of the anti-apoptotic protein Bcl-$X_{L,}$ and decreased levels of the pro-apoptotic proteins Bax, Caspase-3, and PARP. Specifically we will assess cardiomyocyte integrity between groups of mice administered DOX+TRZ and NACA+DOX+TRZ by exploring changes in LV systolic function, histological damage, changes in GATA-4, degree of apoptosis, and lipid peroxidation.

Chapter 4: Methodology

4.1 Animal Procedures

All animal procedures were conducted in accordance with guidelines published by the Canadian Council on Animal Care. All procedures, including drug administration and longitudinal echocardiographic studies, were approved by the Animal Protocol Review Committee at the University of Manitoba.

4.2 Animal Model

For aims 1 and 2, two protocols were followed.

Protocol 1 (Acute *in vivo* 10 day study): A total of 100 mice (7 to 8 week old C57Bl/6 female mice) were randomized to the treatment groups as shown in Figure 6.

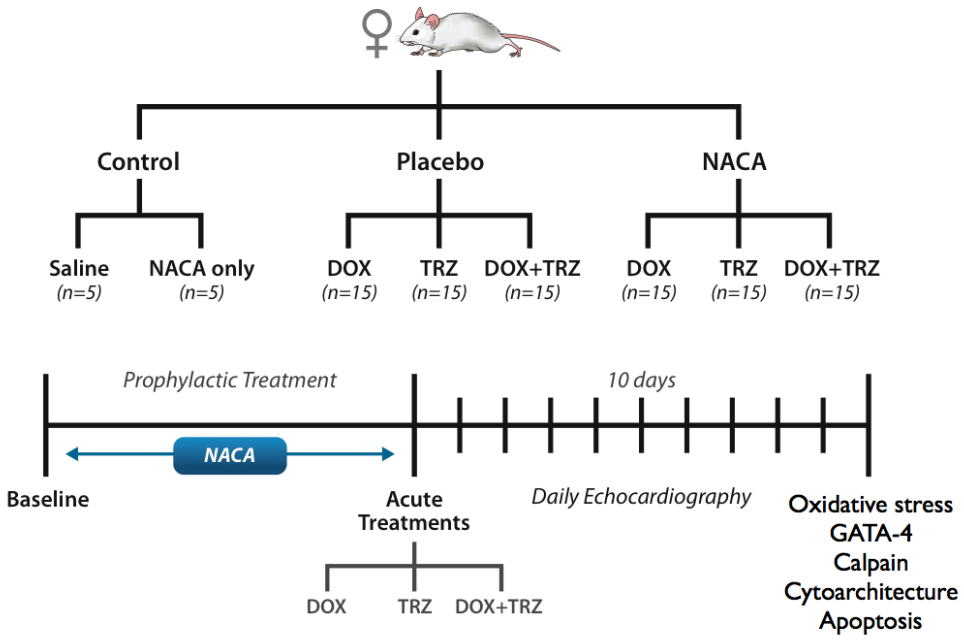

Figure 6: A total of 100 WT C57Bl/6 female mice were randomized to one of the following drug regimens: Saline; NACA (250 mg/kg); DOX (20 mg/kg); TRZ (10 mg/kg); DOX+TRZ; NACA+DOX; NACA+TRZ; and NACA+DOX+TRZ. NACA was administered 30 minutes prior to the experimental arm. Mice received daily echocardiography for 10 days at which point they were euthanized and tissues were extracted for biochemical analysis.

Protocol 2: (Acute *in vivo* 72-hour study): A total of 70 mice (7 to 8 week old C57Bl/6 female mice) were randomized to the treatment groups as shown in Figure 7.

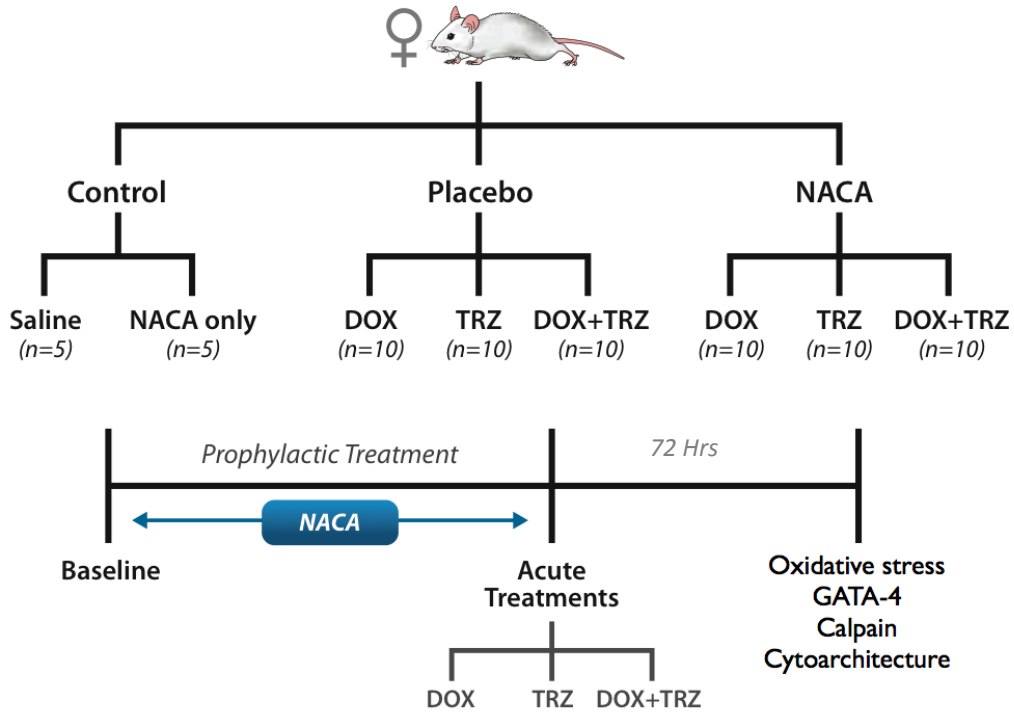

Figure 7: A total of 70 WT C57Bl/6 female mice were randomized to one of the following drug regimens: Saline; NACA; DOX; TRZ; DOX+TRZ; NACA+DOX; NACA+TRZ; and NACA+DOX+TRZ. NACA was administered 30 minutes prior to the experimental arm. Following injection with one of the above drug regimens, the mice were euthanized at 72 hours to allow an early time point for biochemical analysis.

All female mice were quarantined for 1 week prior to being randomized to a treatment arm in both protocols. Prior to receiving one of the anti-cancer regimens and/or NACA, all mice underwent baseline transthoracic echocardiography (TTE) and weight analysis. One time administration (intraperitoneal injection) of 0.9% saline, NACA (250mg/kg)[104], DOX (20mg/kg)[12], TRZ (10mg/kg)[12], DOX (20mg/kg) + TRZ (10mg/kg), NACA (250mg/kg) + DOX (20mg/kg), NACA (250mg/kg) + TRZ (10mg/kg), NACA (250mg/kg) + DOX (20mg/kg) + TRZ (10mg/kg) were administered following baseline data acquisition for both protocols. NACA (250 mg/kg) was administered prophylactically, 30 minutes prior to the chemotherapy drugs. Serial echocardiography and weight measurements were performed daily for 10 days, at which time all surviving mice were anesthetized using pentobarbital (110mg/kg, i.p) and hearts were preserved for histological and biochemical analyses for protocol 1 (Figure 6). For protocol 2, mice were administered the same drug regimens as protocol 1 and weight measurements were performed daily for 72 hours. At 72 hours, mice were euthanized with pentobarbital (110mg/kg i.p.) and hearts were preserved for biochemical and histological analyses (Figure 7). The chemotherapeutic dosages administered to mice are the minimum concentrations required to induce LV systolic dysfunction in a murine model.[13, 14, 109]

4.3 Echocardiography

Non-invasive assessment of cardiac function was performed via murine echocardiography in awake mice at baseline, and daily for a total of 10 days

(Protocol 1). All echocardiographic images were acquired using a 13-MHz probe (Vivid 7, GE Medical Systems, Milwaukee, WI, US). All of the mice were imaged in the parasternal long axis (PLAX) and short axis (SAX) views, as previously described.[12, 13, 110, 111] Images were post-processed offline using the EchoPAC PC software (Vivid 7, version 11.2, GE Medical Systems, Milwaukee, WI, US). Images acquired in the PLAX view were used to calculate LVEF by manually tracing LV end-diastolic and end-systolic volumes (Equation 1). Images acquired in the SAX were used to evaluate LV cavity dimensions through M-mode echocardiography. Parameters used include LV end-diastolic diameter ($LVID_{ED}$), LV end-systolic diameter ($LVID_{ES}$), posterior wall thickness (PW), and interventricular septal thickness (IVS).[12, 13] In addition, the GE EchoPAC PC program was also used to calculate fractional shortening (FS) as described by equation 2.

Equation 1: Calculation of LVEF

$$\text{LVEF} = \frac{LVEDV - LVESV}{LVEDV} \times 100\%$$

Equation 2: Fractional Shortening

$$\text{FS} = \frac{LVEDD - LVESD}{LVEDD} \times 100\%$$

4.4 Histology

The sectioned hearts removed from the thoracic cavity had a tissue sample flash frozen in liquid nitrogen for histological analysis via electron microscopy. These heart sections were fixed with 3% glutaraldehyde in 0.1 M phosphate buffer at pH 7.3 at room temperature for 3 hours. Tissues were rinsed and placed

in 0.1 phosphate buffer containing 5% sucrose at 4° C for 24 hours. Post-fixation following the overnight wash was done at room temperature with 1% osmium tetroxide in 0.01 M phosphate buffer for 2 hours. The tissue samples were then dehydrated in ascending concentrations of ethanol and embedded in Epon 812 using techniques as previously described.[112] Sections were stained with uranyl acetate and lead citrate for viewing and photography with the Philips CM12 electron microscope in order to determine cell integrity. Grids were coded without prior knowledge of their source to eliminate observer bias. Wet to dry weight ratios for liver and lung samples were measured for mice at time of euthanization. Tissue samples were dried for 72 hours at 65° C.

4.5 Immunohistochemistry

At day 10, surviving mice were euthanized and hearts were removed. Each heart was rinsed in 0.9% saline and the apex was collected. The apex was embedded in OCT blocks and stored at -80° C. Preparation for this procedure began by making a fixative for the tissue sections. 2 g paraformaldehyde solution was added to 100 ml of water. The solution was heated for 1 minute with the addition of 10 drops of 1 N NaOH. After heating the solution, it was placed on a stir plate until it dissolved into a homogeneous mixture. The 1% paraformaldehyde solution was brought to a final volume of 200ml in PBS and the pH was adjusted to 7.4. This final solution was filtered through #1 Whatman paper.

The OCT embedded tissues was then mounted to the sectioning apparatus. Frozen tissue sections were sliced at a thickness of 7 μm and placed on a glass microscope slide (superfrost + Fisher). The slides with tissue sections were then placed in the prepared 1% paraformaldehyde fixation solution for 1 minute at 4° C. The tissues were washed with PBS for 5 minutes at a time, for a total of 3 washes. After washing, the tissues were permeabilized with fresh 0.3% Triton X-100 in PBS for 30 seconds. Following permeabilization, 6 wash cycles with PBS for a total of 5 minutes each were performed. Sections probed with mouse antibodies were then incubated at room temperature with MOM IG Block (Vector Laboratories BMK-2202) for 60 minutes (22 μl concentrate/625 ul PBS). Primary antibodies for myosin (MF-20, Developmental Studies Hybridoma Bank), dystrophin (AB 15277, Abcam 1:400), desmin (AB 15200, Abcam 1:20), and connexin-43 (610061 BD Transduction 1:100) were placed on the tissue sections and stored for 24 hours at 4°C. The primary antibody was then washed with PBS (3x5 minutes). Secondary antibody AlexaFluor 488 (A21206, Life Technologies) was placed on the tissue sections left for 60 minutes at room temperature, followed by a 5 minute wash in PBS. Sections were stained with Hoechst 33342 nucleic acid stain (Calbiochem cat# 382065). 5 final washes for 5 minutes each were performed with PBS before mounting tissue sections with Prolong Gold mounting media (Invitrogen without DAPI) to cover slips onto the tissue-sectioned slides. Slides of tissue sections were than analyzed using the Zeiss Axiovert 200 M with Epifluorescence microscope. The sections were viewed and photographed with Axiovision 4.8.2 software.

4.6 High Pressure Liquid Chromatography – Mass Spectrometry for Oxidized Phospholipids

Tissue sections from surviving mice were stored for lipid analysis. A section of cardiac tissue was stored in a vial containing PBS (pH 7.4) with EDTA and the addition of gaseous nitrogen infused into the tube, stored at -80°C. In order to perform high-pressure liquid chromatography, extraction of lipids from cardiac tissue was done by the described method.[113] Frozen tissues were weighed at 10-20 mg. These tissues were placed in mortar with the addition of 2-3 ml of liquid nitrogen in order to create a tissue powder. The powdered tissues were placed in 15 ml falcon tubes with the addition of 6 ml ice cold C-M (C-M mixture, 2:1 vol/vol, 0.01% BHT). Once mixed, 0.1 ml of internal standards was added to the mixture, followed by a gentle vortex and addition of 1.5 ml of PBS. This mixture was then centrifuged at 4°C at 3500 RPM for 5 minutes. The mixture was separated using a Pasteur pipette placed through the aqueous phase and interfacial protein residue and finally into the lipid phase which was withdrawn and placed into another centrifuge tube. The remaining aqueous phase mixed with protein residue was mixed with 4.5 ml of C-M-PBS (86:14:1) and centrifuged again at 4° C at 3500 RPM for 5 minutes. The lipid extraction with the Pasteur pipette was repeated. The solvents were evaporated from the extracts by use of the nitrogen evaporator. The lipid extracts were placed in 0.5 ml of C-M (2:1) and transferred to a sampling vial stored with infusion of nitrogen gas at 80° C.

The lipid extracts were reconstituted in the reverse phase solvent system consisting of acetronitrile/isopropanol/water (65:30:5 v/v/v). 0.03 ml samples

were injected into the Ascentis Express C18 column (15cmx2.1mm, 2.7 µm; Supelco Analytical, Bellofonte, PA 16823-0048 USA) using an HPLC system (Shimadzu USA MFG Inc). This apparatus uses a DGU-20A3 degasser, LC-20-AD pumps, SIL-20AC HT auto sampler and CTO-20 AC column oven. The temperature of the auto sampler and column oven were left at 4°C and 45°C, respectively. This HPLC system was attached to 4000 QTrap Triple Quadrupole Linear Ion Trap Mass Spectrometer system equipped with Turbo V electrospray ion source (Absciex, 500 Old Connecticut Path, Framingham MA 01701 USA).

Elutions were performed via linear gradient of solvent A (Acetonitrile-Water, 60:40 vol/vol) and solvent B (Isopropanol-Acetonitrile, 90:10, vol/vol). Both of the solvents contained 10 mM of ammonium formate and 0.1% formic acid. The time format used was 0.01 min 32% B; 1.50 min 32% B; 4.0 min 45% B; 5.0 min 52% B; 8.0 min 58% B; 11.0 min 55% B; 14.0 min 70% B; 18 min 76% B; 21.0 min 97% B; 25.0 min 97% B; 25.1 min 32% B; and 30.0 min 32% B. The elution was stopped at 30.1 minutes with a flow rate of the mobile phase at 0.26 ml/min. The quantification of data was done by using Multiquant 2.1.

4.7 Western Blotting

Frozen heart tissues were placed in a mortar with the addition of liquid nitrogen and ground into powder. Ground tissues were placed in solution with radioimmunoprecipition (RIPA) buffer containing protease and phosphatase inhibitors (Thermo Scientific). These samples were cooled on ice for 20 minutes and then centrifuged at 10, 000 RPM at 4° C for 10 minutes. The resulting supernatant was removed and extracted proteins were quantitated using the

BioRad protein assay. Protein lysates were stored in pre-chilled labeled tubes at -80°C until needed.

Stored protein lysates were used for Western Blot analyses. 30 µg of protein were loaded in each lane and samples were electrophoresed in a 12% sodium dodecyl sulfate polyacrylamide gel (SDS-PAGE) at 100 V for 1.5 hours using the Mini-PROTEAN Tetra System (BioRad) at room temperature. Once separated, proteins were transferred to a 0.45 mm PVDF membrane (Roche Diagnostics) for 2 hours at 100V at 4° C. The protein embedded membranes were stained with Ponceau S to ensure that the transfer was effective and to validate equivalent total protein loading between lanes. Once analyzed, the membrane was washed with 1X Tris Buffered Saline with 0.1% Tween 20 (TBST). Membranes were blocked for 1 hour in 1X BSA blocking buffer/TBST (Thermo Scientific), which was reconstituted form the 10X stock solution that was previously prepared. Membranes were placed in plastic holders with the addition of primary antibodies for a total of 24 hours at 4° C. The membranes were washed 3X for 10 minutes with 1X TBST and then placed in secondary antibody for 45 minutes at room temperature. Membranes were again washed 3X for 10 minutes with 1X TBST. Proteins in the membrane were detected using the ECL Plus Detection Reagent (Western Lighting Plus-ECL, Amersham) with the use of X-ray film exposure. Primary antibodies used include the polyclonal antibodies to Bax, Bcl-xL Caspse-3, and PARP (Cell Signlaing), which were all probed for individually. GAPDH polyclonal antibody was used as a loading control (Sigma).

Stripping of proteins was achieved by placing the membrane into Restore PLUS Western Blot Stripping Buffer (Thermo Scientific) for 15 minutes at room temperature. Following the stripping buffer, membranes were washed with 1 X TBST for a total of 3 washes, and then probed with a primary antibody for GAPDH for 15 minutes. Band intensity was quantitated using the image analysis software Quantity One; BioRad Laboratories, Inc).

4.8 Quantitative Real Time PCR

Harvested cardiac tissue from surviving mice was also extracted for RNA analyses. The genes of interest included the pro-apoptotic proteins; Caspase-3, PARP, Bax, the anti-apoptotic protein Bcl-xL, and the cardiac transcription factor GATA-4. GAPDH was used as a housekeeping gene (Table 1) shows the designed primer sequences for these genes and the corresponding amplicon sizes). RNA was extracted from the tissues using with the Qiagen RNA isolation kit (cat# 74704, RNeasy® Fibrous Tissue Mini Kit). The 12-step protocol allowed the successful extraction of RNA from the heart tissues from the euthanized mice. The extracted RNA was measured for purity and concentration by using the NanoDrop Lite Spectrophotometer (Thermo Scientific) and the sample purity was evaluated by the 260/280 nm ratio.

A total of 25-50 ng of RNA were ran by qPCR (quantitative Real Time PCR) using the q-script 1 step qPCR kit (cat# 95057, Quanta Biosciences) with a protocol as per the manufacturer's instructions; the composition of the reaction mix is shown in Table 2. Prior optimization by test runs was done for the

determination of a number of conditions, namely, the best primer pair (Table 1), the optimal annealing temperature (using gradient PCR) and the optimal amount of RNA which resulted in doubling the amplicon efficiently. Real time PCR was ran using the BioRad iQ5 optical system and analyzed by the BioRad software (Bio-Rad Labs, CA). The optimized PCR conditions comprised of an initial 2 min activation of Polymerase at 94°C, followed by 40 cycles of denaturation (15 secs, 94°C), annealing (2 secs, 54°C) and extension (20 secs, 72°C) respectively. Expression was calculated from the threshold cycle (Ct,) of each transcript.

The relative expression was calculated by the $2^{-\Delta\Delta Ct}$ method[114]. Data analysis was done as described[115]. All data were normalized to the housekeeping gene, GAPDH. Normalized values were expressed as fold change in expression relative to the saline control. The PCR products were reconfirmed by melt curve analysis and gel electrophoresis respectively. All values are an average of three independent experiments and were expressed as mean ± S.E.M.

Target Gene	Forward Primer	Reverse Primer
Bax 152 Bp	5'CTTTTTGCTACAGGGTTTCATCCAG3'	5'CCATATTGCTGTCCAGTTCATCTCC3'
Bcl-xL 161 Bp	5'TCTAACATCCCAGCTTCACATAACC3'	5'CCTGCATCTCCTTGTCTACGCTTT3'
Caspase-3 181 Bp	5'TTTGTCCCATAAATGACCCCTTCAT3'	5'CAGCCAACCTCAGAGAGACATTCAT3'
PARP 214 Bp	5'GGAAGTCCTCACACACAACTCGAAC3'	5'AAGCCCCTGTCTAACATGAAGATCC3'
GATA-4 161 Bp	5'AACCCTGGAAGACACCCCAATCT3'	5'TTGATGCCGTTCATCTTGTGATAGA3'
GAPDH 127 Bp	5'AATTGTGAGGGAGATGCTCAGTGTT3'	5'CAATGAATACGGCTACAGCAACAGG3'

Table 1: Forward and Reverse Primers for quantitative real time PCR for target genes of interest.

qPCR Reaction Mix	Final Concentrations	Volume
Sybr Green Mix	1X	12.5 ul
Forward Primer	200 nM	0.5 ul
Reverse Primer	200 nM	0.5 ul
RNA	10 ng/µl	25-50 ng (equivalent volume)
Reverse Transcriptase	25 ul	0.5 ul
H_2O	----------	(in accordance with RNA amount)
Total volume	----------	25 µl

Table 2: qPCR reaction mix content.

4.9 Statistical Analysis

All data are expressed as mean±SD. Statistical significance of echocardiographic findings was assessed using a 1 (Genotype) x 2 (Time) mixed factorial design with repeated measurements for the factor of time. Post-Hoc analysis was achieved through repeated measures of ANOVA in order to evaluate the significance between independent factors. Post-Hoc between group analyses were conducted via the Levene's test in order to assess homogeneity between group variances. P-values for main effects and interactions were recorded when appropriate. Histological data analysis involved non-parametric comparison of scores ranging from 1-4, calculated using the Mann-Whitney test, with 4 being indicative of severe damage. A p value of <0.05 was considered significant.

Biochemical and western blot data was analyzed via Student-t tests, with p-values of <0.05 considered significant. The statistical analysis package SPSS 15.0 and Graphpad Prism 5 were used to perform these analyses.

Chapter 5: Results

Protocol 1: 10 Day Results

5.1 Murine Echocardiography (Protocol 1: 10 Day Study)

Baseline values for LV dimensions and systolic function, as determined by fractional shortening (FS) and ejection fraction (EF) were similar in all mice. Heart rate measurements of all mice at baseline were within the normal limits as baseline. The data for all of these parameters at baseline and day 10 are presented in Table 3.

Echo Variable	Group	Baseline	Day 10	P-Value
HR (beats/min)	Saline	694±8	683±9	0.82
	NACA	675±11	690±10	0.78
	DOX	687±12	682±5	0.77
	NACA+DOX	689±10	691±8	0.65
	TRZ	705±15	702±11	0.86
	NACA+TRZ	704±12	695±9	0.87
	DOX+TRZ	701±8	689±12	0.78
	NACA+DOX+TRZ	688±11	693±7	0.70
PWT (mm)				
	Saline	0.81±0.02	0.82±0.01	0.83
	NACA	0.80±0.01	0.82±0.02	0.86
	DOX	0.82±0.02	0.82±0.01	0.91
	NACA+DOX	0.83±0.02	0.82±0.03	0.82
	TRZ	0.81±0.02	0.81±0.01	0.83
	NACA+TRZ	0.80±0.01	0.80±0.02	0.85
	DOX+TRZ	0.82±0.03	0.82±0.04	0.92
	NACA+DOX+TRZ	0.81±0.02	0.80±0.02	0.80
LVEDD (mm)				
	Saline	3.2±0.1	3.1±0.2	0.89
	NACA	3.1±0.1	3.2±0.1	0.76
	DOX	3.2±0.2	3.9±0.2*	<0.05
	NACA+DOX	3.1±0.1	3.4±0.1*#	<0.05
	TRZ	3.1±0.2	3.2±0.2	0.76
	NACA+TRZ	3.1±0.2	3.2±0.2	0.82
	DOX+TRZ	3.2±0.1	4.3±0.2*	<0.05

	NACA+DOX+TRZ	3.2±0.2	3.6±0.1*#	<0.05
LVEF (%)				
	Saline	72±4	73±4	0.87
	NACA	74±2	73±1	0.82
	DOX	73±4	43±2*	<0.05
	NACA+DOX	73±4	62±3*#	<0.05
	TRZ	71±4	72±3	0.88
	NACA+TRZ	73±4	73±1	0.68
	DOX+TRZ	73±4	32±2*	<0.05
	NACA+DOX+TRZ	72±4	55±3*#	<0.05
FS (%)				
	Saline	50±2	52±2	0.86
	NACA	51±2	52±1	0.88
	DOX	50±4	41±2*	<0.05
	NACA+DOX	52±3	45±3*#	<0.05
	TRZ	52±4	53±3	0.82
	NACA+TRZ	54±2	51±2	0.78
	DOX+TRZ	52±2	34±3*	<0.05
	NACA+DOX+TRZ	54±3	41±3*#	<0.05

Table 3: Echocardiographic findings at baseline and day 10 in C57Bl/6 female mice receiving one of the drug regimens listed. Analyses included assessment of heart rate (HR), posterior wall thickness (PWT), left ventricular end diastolic diameter (LVEDD), and left ventricular ejection fraction (LVEF). Values presented are mean±SEM from an n=5 Saline, n=5 NACA, n=15 DOX, n=15 NACA+DOX, n=15 TRZ, n=15 NACA+TRZ, n=15 DOX+TRZ, n=15 NACA+DOX+TRZ.
* $p<0.05$ Saline VS Treatment
# $p<0.05$ DOX VS NACA+DOX and DOX+TRZ VS NACA+DOX+TRZ

The LVEDD was normal in all of the treatment groups at baseline, as seen in Table 3. In mice receiving DOX alone, the LVEDD increased significantly from 3.2±0.2 at baseline to 3.9±0.2 at day 10 ($p<0.05$). Mice that received the combination treatment of DOX+TRZ similarly showed a significant increase in LVEDD from 3.2±0.1 at baseline to 4.3±0.2 at day 10 ($p<0.05$). The prophylactic administration of NACA attenuated the increase in LVEDD in both the DOX and DOX+TRZ treated mice at day 10, respectively ($p<0.05$) (Figure 8).

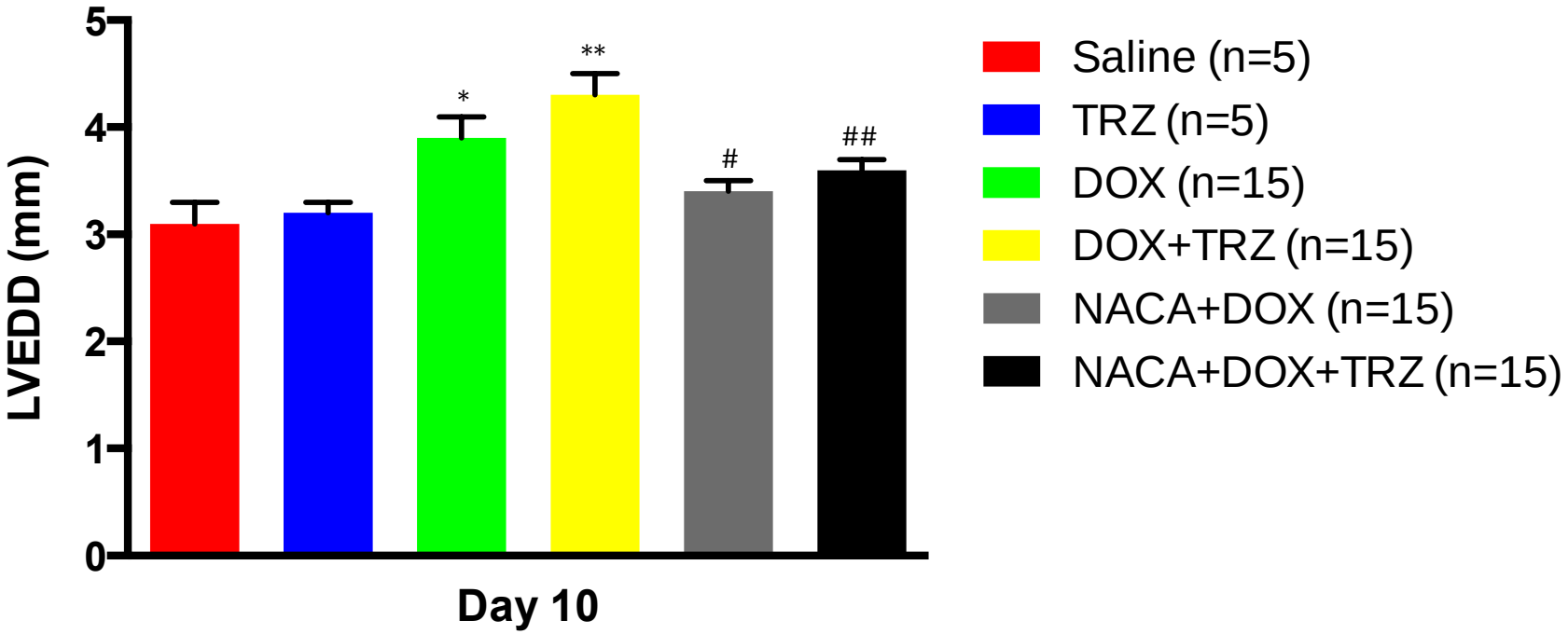

Figure 8: The LVEDD of groups of wild type C57Bl/6 female mice at day 10. In wild type mice receiving saline, there was no significant difference in LVEDD at baseline and 10 days of follow-up. In WT female mice receiving DOX alone, LVEDD increased from 3.2±0.2 at baseline to 3.9±0.2 at day 10 ($p<0.05$). In WT female mice receiving the combination of DOX+TRZ, LVEDD increased from 3.2±0.1 at baseline to 4.3±0.2 at day 10 ($p<0.05$). Prophylactic administration of NACA to WT female mice receiving either DOX alone or DOX+TRZ was cardioprotective with an LVEDD of 3.4±0.1and 3.6±0.1 at day 10 ($p<0.05$), respectively.

* $p<0.05$ Saline VS DOX

** $p<0.05$ Saline VS DOX+TRZ and DOX VS DOX+TRZ

# $p<0.05$ DOX VS NACA+DOX

$p<0.05$ DOX+TRZ VS NACA+DOX+TRZ and NACA+DOX VS NACA+DOX+TR

LVEF was within normal limits in the various treatment groups at baseline as seen in table 3. In mice treated with DOX, LVEF decreased from 73±4 at baseline to 43±2 at day 10 ($p<0.05$). This drop in LVEF was even more pronounced in mice receiving the combination of DOX+TRZ, with baseline measurements of 73±4 as compared to day 10 values of 32±2. The prophylactic administration of NACA attenuated the drop in EF in both the DOX and DOX+TRZ treated mice at day 10, respectively ($p<0.05$) (Figure 9).

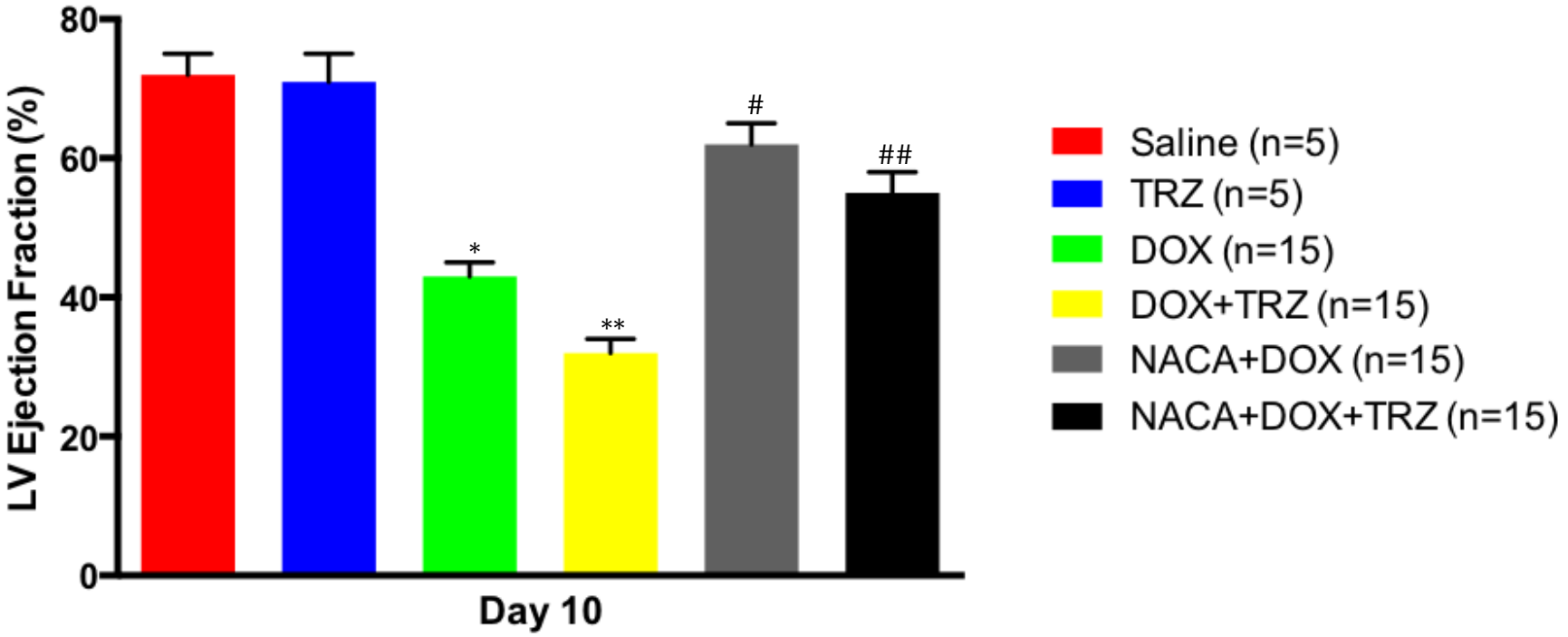

Figure 9: The LVEF of groups of wild type C57Bl/6 female mice at day 10. In wild type mice receiving either saline or TRZ alone, there was no significant difference in LVEF at baseline and 10 days of follow-up. In WT female mice receiving DOX alone, LVEF decreased from 75±2% at baseline to 43±2% at day 10 ($p<0.05$). In WT female mice receiving the combination of DOX+TRZ, LVEF decreased from 75±3% at baseline to 32±2% at day 10 ($p<0.05$). Prophylactic administration of NACA to WT female mice receiving either DOX alone or DOX+TRZ was cardioprotective with an LVEF of 62±3% and 55±3% at day 10 ($p<0.05$), respectively.

* $p<0.05$ Saline VS DOX

** $p<0.05$ Saline VS DOX+TRZ and DOX VS DOX+TRZ

# $p<0.05$ DOX VS NACA+DOX

$p<0.05$ DOX+TRZ VS NACA+DOX+TRZ and NACA+DOX VS NACA+DOX+TRZ

5.2 Immunohistochemistry: Structural Integrity (Protocol 1: 10 Day Study)

There was no significant changes in the cellular structural integrity at day 10 via immunohistochemistry. Structural integrity was assessed through analysis of key proteins including desmin (cytoskeleton), dystrophin (subsarcolemmal integrity), myosin (myofibrillar integrity), and connexin-43, representing the main intercellular communication channel. Changes in these proteins were further compared through western blot analyses. Changes between groups were evaluated to determine if DOX, TRZ, or the combination of DOX+TRZ would affect their relative levels, and whether NACA would prevent these changes. No significant changes were observed between the various treatment groups through analyses of western blots as seen in Figure 10.

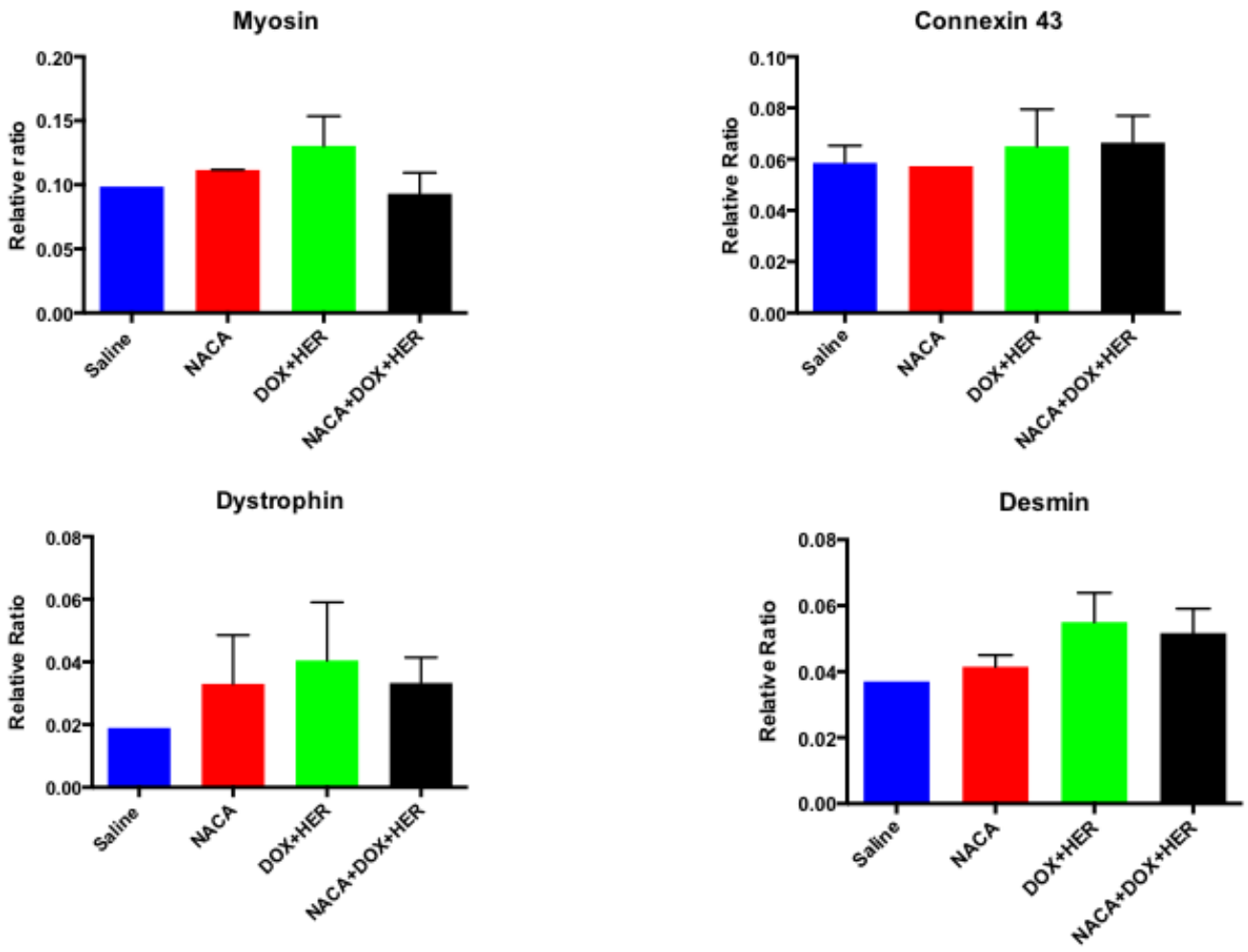

Figure 10: Muscle protein analysis in C57Bl/6 female mice at day 10. Treatment groups include Saline (n=2), NACA (n=2), DOX+HER (n=5), and NACA+DOX+HER (n=5). No changes were observed between the various treatment arms at day 10 in any of the groups

5.3 Superoxide Production (Protocol 1: 10 Day Study)

Superoxide production measured by lucigenin-enhanced chemiluminescence confirmed that superoxide production increased 3-fold and 4-fold in hearts of wild type C57Bl/6 female mice treated with either DOX or DOX+TRZ respectively. The prophylactic administration of NACA reduced the degree of OS in both groups of mice (DOX and DOX+TRZ) as seen in Figure 11.

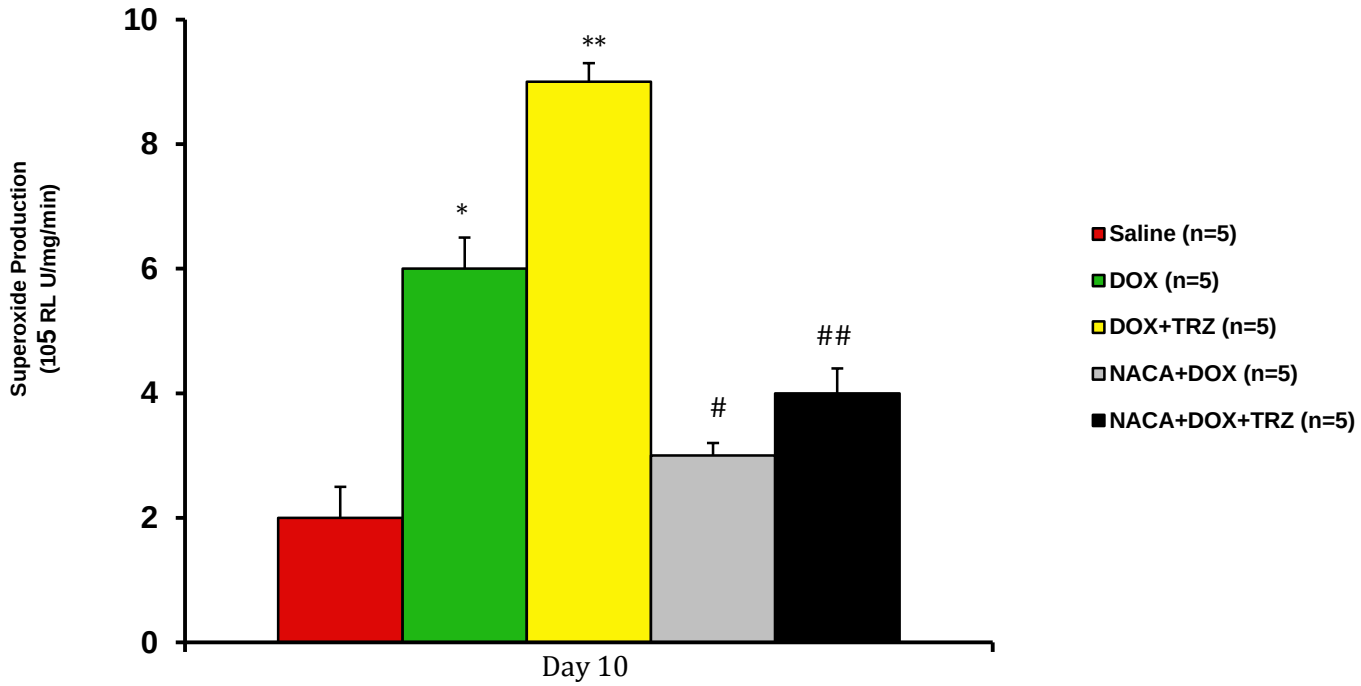

Figure 11: A total of 25 WT female mice (n=5 per group) were treated with either 0.9% saline, DOX, DOX + TRZ, NACA + DOX, or NACA+DOX+TRZ. NACA injections were administered 30 minutes prior to the experimental arm. Cardiac tissue was harvested at 24 hours for measurement of superoxide production using lucigenin-enhanced chemiluminescence at day 10.
* $p<0.05$ Saline VS DOX
** $p<0.05$ Saline VS DOX+TRZ and DOX VS DOX+TRZ
# $p<0.05$ DOX VS NACA+DOX
$p<0.05$ DOX+TRZ VS NACA+DOX+TRZ and NACA+DOX VS NACA+DOX+TRZ

5.4 Western Blotting – Apoptotic Analyses (Protocol 1: 10 Day Study)

Heart tissues extracted from euthanized mice at day 10, were assessed for protein expression of key molecular markers involved in apoptosis. In mice receiving DOX or DOX+TRZ, the expression of caspase-3 (36 kDa) was increased to 1.2 and 1.6 (relative ratio) respectively (Figure 12). The prophylactic administration of NACA significantly decreased the expression of 36 kDa caspse-3 in both groups to 0.9 and 1.05 (relative ratio) respectively (Figure 12).

Similarly, the degree of apoptosis was also assessed by the Bax/Bcl-xL ratio. In mice receiving DOX or DOX+TRZ the Bax/Bcl-xL ratio was 1.5 and 1.86 (fold activation) respectively (Figure 13). The prophylactic administration of NACA significantly decreased the ratio in both groups to 1.25 and 1.4 (fold activation) respectively (Figure 13).

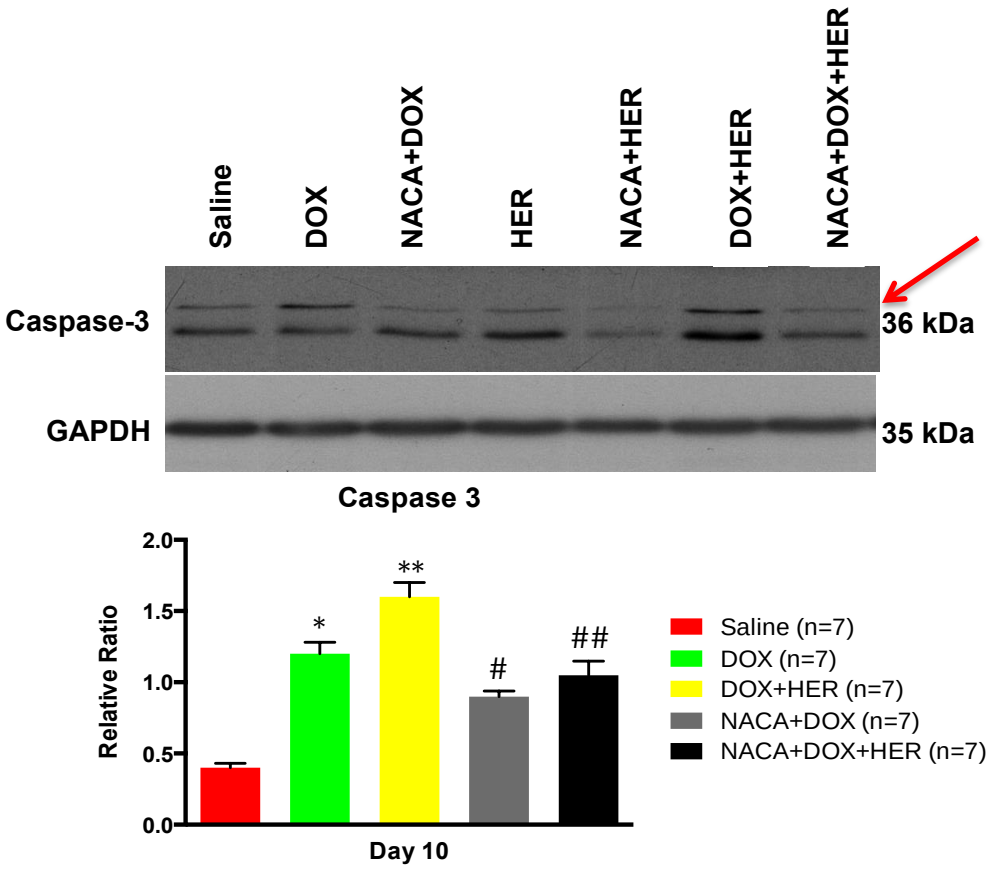

Figure 12: The average Caspase-3 protein expression at day 10 expressed as a relative ratio in C57Bl/6 mice treated with 0.9% saline (n=7), DOX (n=7), DOX+HER (n=7), NACA+DOX (n=7), NACA+DOX+HER (n=7). Prophylactic NACA administration decreased caspase-3 levels in both groups. The top band (36 kDa) was used during quantification of Caspase-3.

* $p<0.05$ Saline VS DOX

** $p<0.05$ Saline VS DOX+TRZ and DOX VS DOX+TRZ

# $p<0.05$ DOX VS NACA+DOX

$p<0.05$ DOX+TRZ VS NACA+DOX+TRZ and NACA+DOX VS NACA+DOX+TRZ

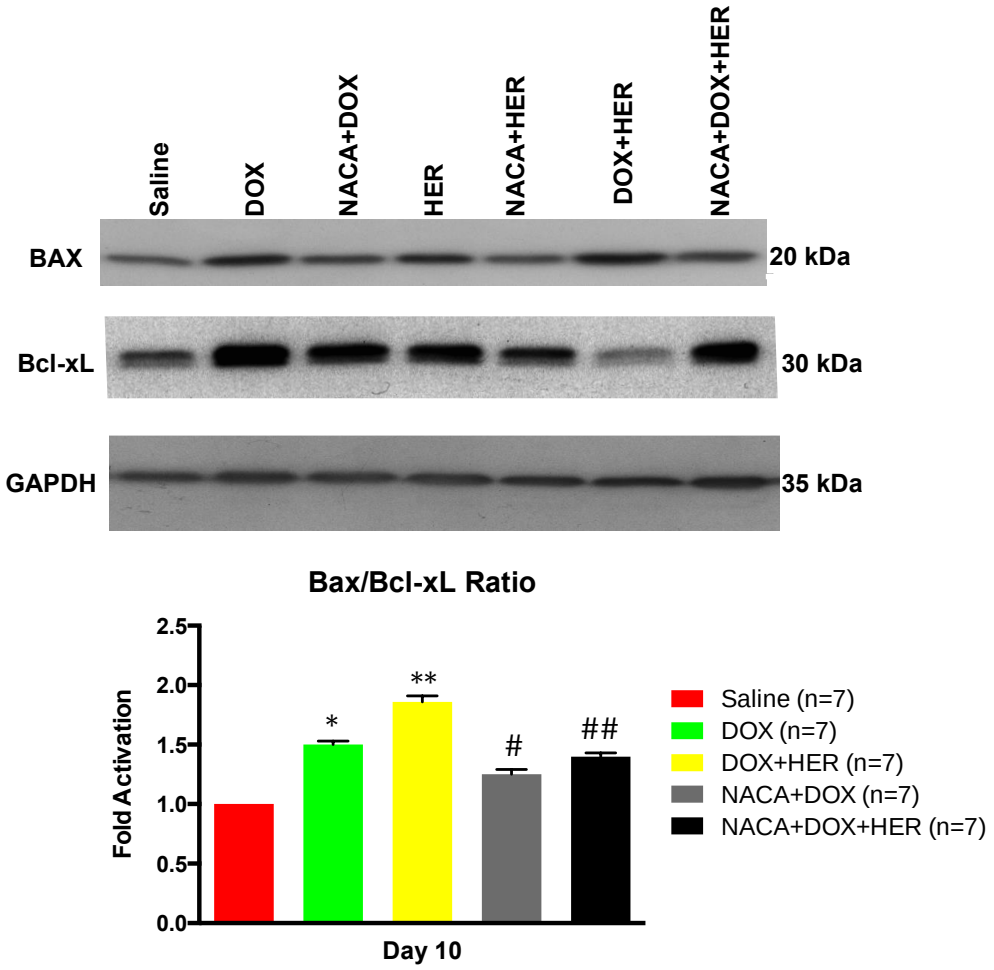

Figure 13: The average Bax/Bcl-xL ratio expression, at day 10 shown as fold activation in C57Bl/6 mice treated with 0.9% saline (n=7), DOX (n=7), DOX+HER (n=7), NACA+DOX (n=7), NACA+DOX+HER (n=7). Prophylactic NACA administration attenuated the degree of apoptosis in both groups.
* $p<0.05$ Saline VS DOX
** $p<0.05$ Saline VS DOX+TRZ and DOX VS DOX+TRZ
# $p<0.05$ DOX VS NACA+DOX
$p<0.05$ DOX+TRZ VS NACA+DOX+TRZ and NACA+DOX VS NACA+DOX+TRZ

Protocol 2: 72 Hour Results

5.5 Histology: Electron Microscopy (Protocol 2: 72 Hour Study)

There was no evidence of myofibril degradation and vacuolization in the saline treated groups at 72 hours post treatment (Figure 13). Histological manifestations of cardiac injury were apparent in WT mice treated with DOX+TRZ, as indicated by myofibril degradation and vacuolization in the electron micrographs (Figure 14). This damage was attenuated in groups of WT mice receiving prophylactic NACA 30 minutes prior to DOX+TRZ drug injection (Figure 14). Histological data analysis involved non-parametric comparison of scores ranging from 1-4, calculated using the Mann-Whitney test, with 4 being indicative of severe damage.

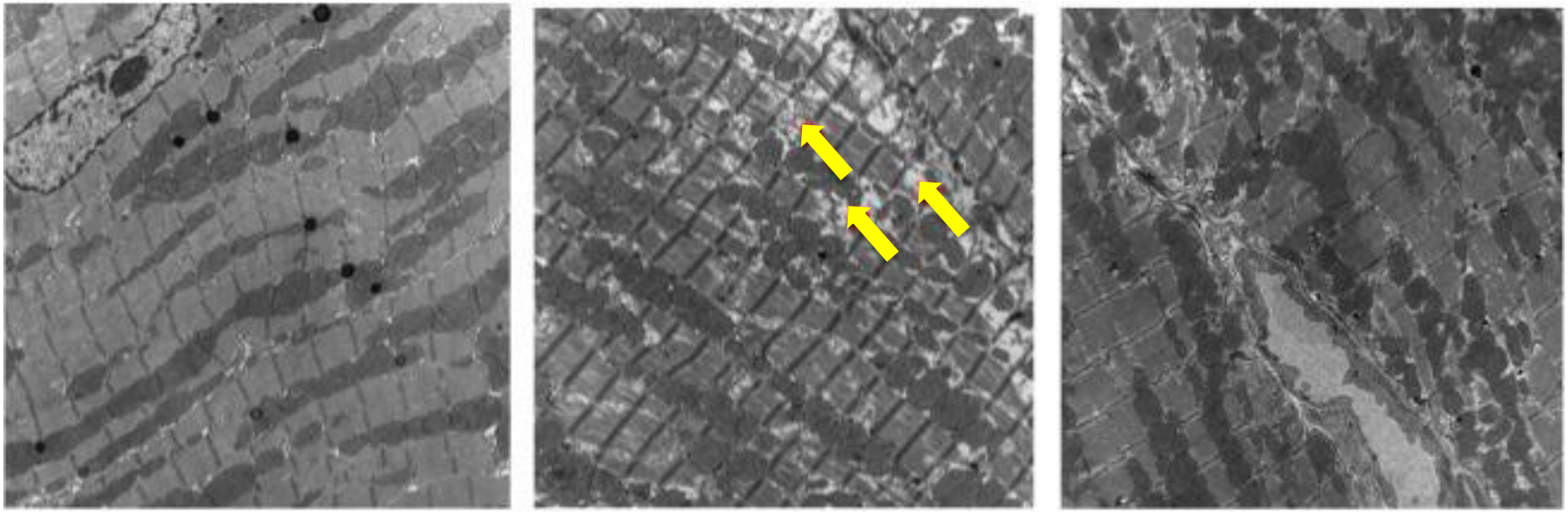

Figure 14: Electron microscopy of representative samples from WT female mouse hearts treated with saline (n=5), DOX+TRZ (n=5), or NACA+DOX+TRZ (n=5) at 5800X magnification. Arrows indicate cardiomyocytes displaying myofibril disarray which was most pronounced in DOX+TRZ treated mice signified by a damage score of 4. The prophylactic administration of NACA was able to attenuate this damage signified by a damage score of 2.

5.6 Oxidized Phospholipid Analyses (Protocol 2: 72 Hour Study)

Heart tissues extracted from euthanized mice at 72 hours (post treatment) were used to assess for the degree of oxidized phospholipids. Analyses included quantification of fragmented oxidized phospholipids. In mice receiving saline, the amount of fragmented oxidized phospholipids was 1.37 ng/mg. Mice receiving DOX or DOX+TRZ had 4.81, and 5.07 ng/mg of fragmented oxidized phospholipids, respectively (Figure 15). The prophylactic administration of NACA was able to decrease the oxidation of fragmented phospholipids in both groups to 2.62 and 1.42, respectively (Figure 15).

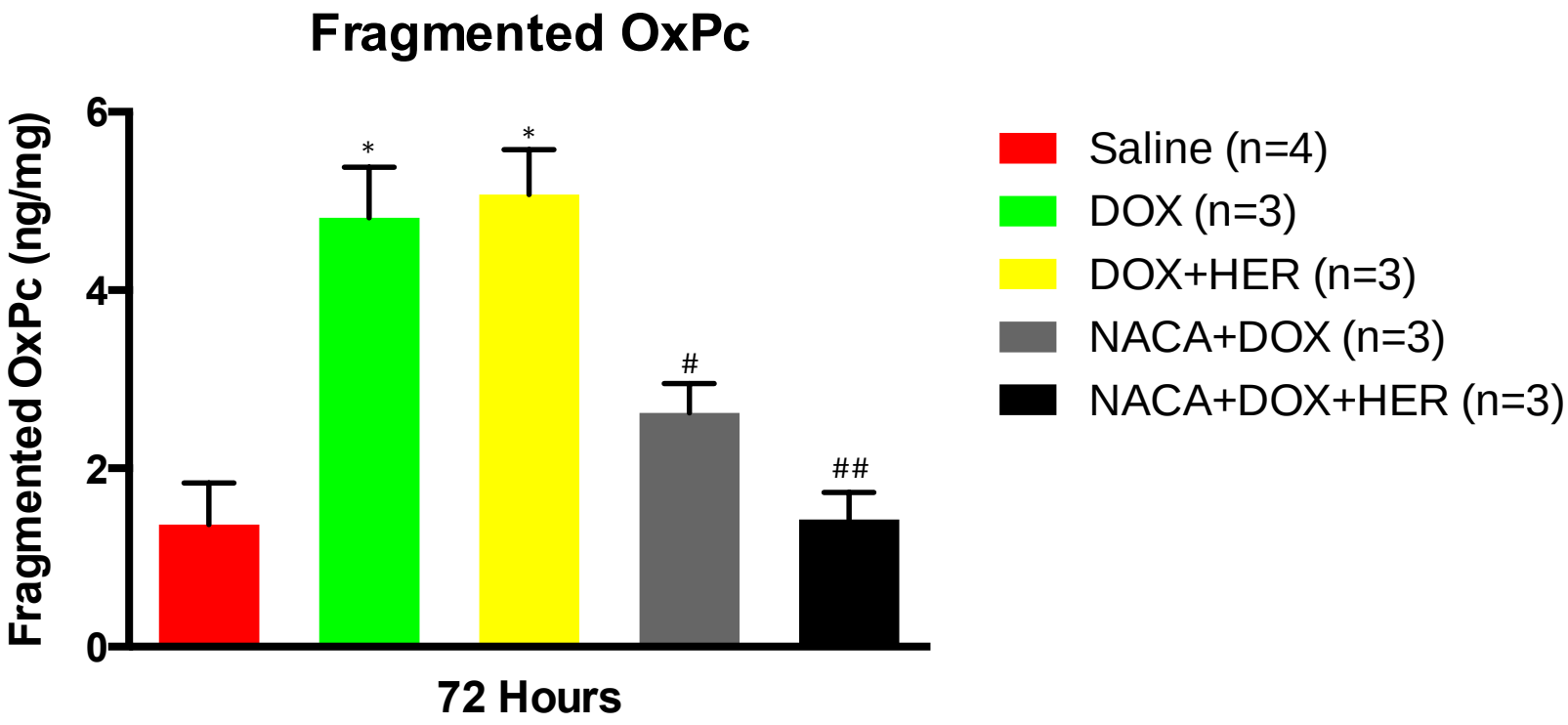

Figure 15: The amount of fragmented oxidized phospholipids (ng/mg) at 72 hours, in C57Bl/6 female mice treated with 0.9% saline (n=4), DOX (n=3), DOX+HER (n=3), NACA+DOX (n=3), NACA+DOX+HER (n=3). Prophylactic NACA administration attenuated the degree of oxidation in both groups.
* $p<0.05$ Saline VS DOX and Saline VS DOX+HER
# $p<0.05$ DOX VS NACA+DOX
$p<0.05$ DOX+TRZ VS NACA+DOX+TRZ and NACA+DOX VS NACA+DOX+TRZ

5.7 qPCR: RNA Analyses (Protocol 2: 72 Hour Study)

Heart tissues extracted from euthanized mice at 72 hours (post treatment) were used to assess for changes in RNA levels for key molecular markers involved in DOX+TRZ mediated cardiac dysfunction. The markers assessed include the apoptotic genes Bax/Bcl-xL, Caspase 3, and PARP. We also assessed changes in the mammalian cardiac transcription factor GATA-4. There were no significant differences from the qPCR analyses of these genes (Figure 16).

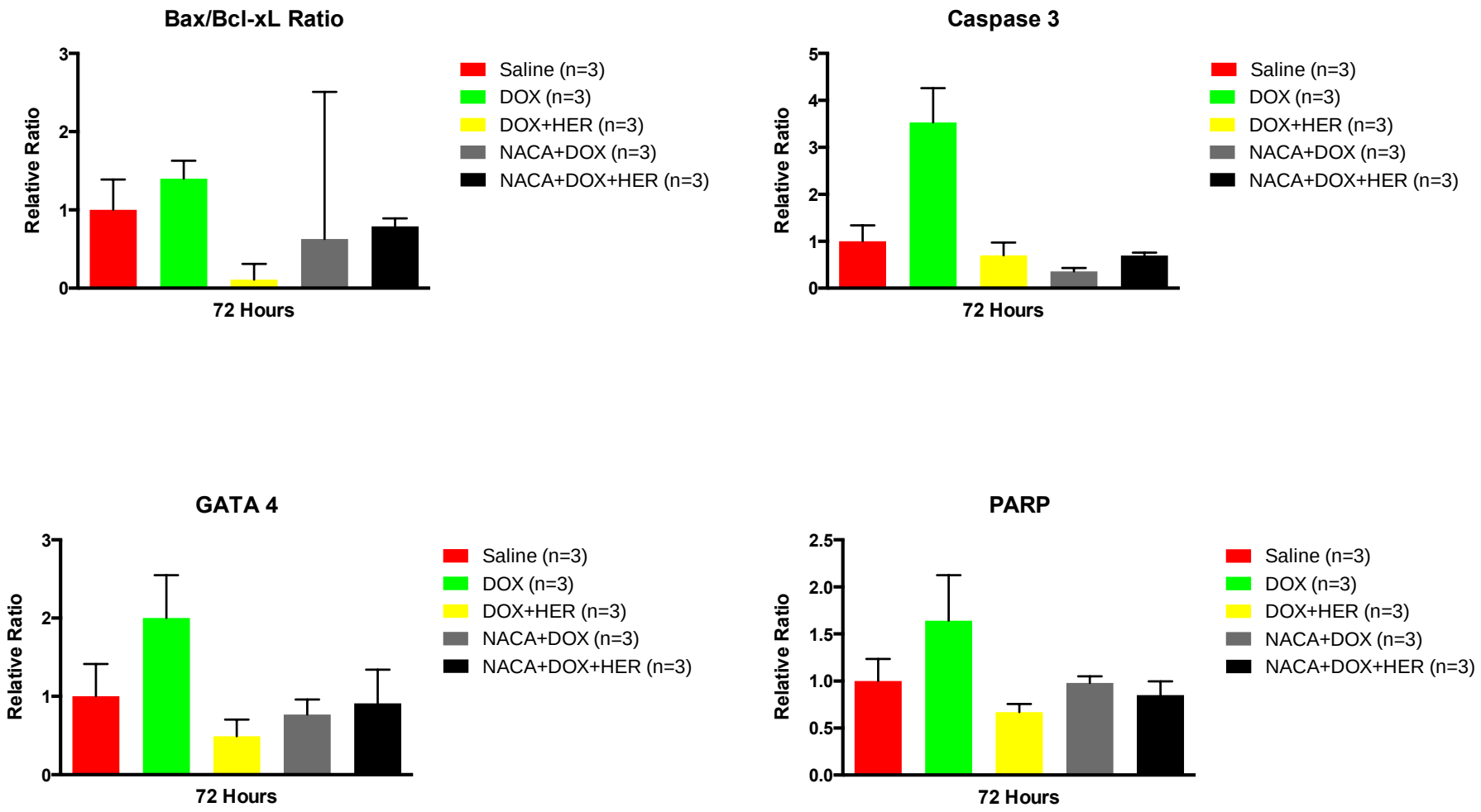

Figure 16: RNA analyses in C57Bl/6 female mice at 72 hours post treatment. Treatment groups include Saline (n=3), DOX (n=3), DOX+HER (n=3), NACA+DOX (n=3), and NACA+DOX+HER (n=5). No significant changes were observed between the various treatment arms for any of the markers at 72 hours post treatment.

Chapter 6: Discussion

6.1 General

The emergence of the novel discipline of Cardio-Oncology has led to advancements in the prevention, diagnosis, and management of cancer patients who develop cardiovascular complications as a result of their cancer treatment. DOX+TRZ are two anti-cancer agents used in the breast cancer setting that are known to reduce overall patient morbidity and mortality, but their clinical use is limited due to their cardiotoxic side effects. A number of previous studied have evaluated the prophylactic role of iron chelation, β-blockers, ACE inhibitors, and anti-oxidants (including Probucol) in the prevention of chemotherapy induced cardiac dysfunction.[13, 116] Our study is the first to formally evaluate the cardioprotective effects of the novel anti-oxidant NACA in a female murine model of DOX+TRZ mediated cardiac dysfunction.

Our study demonstrated that the prophylactic treatment with the anti-oxidant NACA significantly attenuated the cardiotoxic side effects of the combination therapy with Doxorubicin and Trastusuzmab in an acute female murine model of chemotherapy induced cardiomyopathy. In the current study, we demonstrated that NACA: i) prevents adverse left ventricular remodeling due to DOX+TRZ; ii) prevents histological evidence of myofibrillar disarray; iii) reduces the degree of OS as early as 72 hours which extends to day 10 following treatment with DOX+TRZ; and iv) attenuates the degree of cardiac apoptosis.

6.2 Cardiovascular remodeling: Echocardiography

In clinical practice, serial monitoring of LVEF using non-invasive cardiac imaging is the single most important diagnostic tool in the detection of cardiac dysfunction among cancer patients. Once heart failure develops in the setting of a reduced LVEF, however, irreversible cardiac injury may occur.[21, 117] In the emerging field of Cardio-Oncology, a number of basic science studies have evaluated the role of cardiac imaging for the early detection of LV systolic dysfunction due to DOX+TRZ.[12-14, 118]

In an acute murine model of DOX mediated carditoxicity, Neilan *et al.* explored the acute cardiotoxic side effects of this anti-cancer agent.[119] Their study concluded that mice treated with DOX developed early LV cavity dilatation with a LVEDD of 3.2±1 at baseline to 3.4±1 by day 5.[119] Additionally, mice treated with DOX demonstrated a decrease in LVEF of 78±2 % at baseline to 66±3 % at day 5.[119]. The results from their chronic model evaluating DOX mediated cardiotoxicity over 16 weeks were also congruent with their acute model, in which WT mice treated with DOX showed echocardiographic evidence of a dilated cardiomyopathy.[119]

In 2009, Jassal *et al.* expanded on this finding, studying the combined cardiotoxic effects of DOX+TRZ in an acute murine model of cardiomyopathy. Specifically, WT male mice treated with DOX+TRZ had a significant decrease in LVEF from 75 ± 2% to 63 ± 2% at day 4.[12] A recent study by Walker *et al.* from 2011 also reported that mice receiving DOX had a significant increase in left ventricular end diastolic diameter (LVEDD) from 3.2 ± 0.1 mm at baseline to 3.8 ± 0.2 mm at day 10.[13] The combination treatment with DOX+TRZ resulted in an increase in the

LVEDD from 3.1 ± 0.1 mm at baseline to 4.1 ± 0.2 mm by day 10.[13] Of interest, prophylactic treatment with the anti-oxidant Probucol demonstrated a cardioprotective effect by attenuating the increase in LVEDD to 3.1 ± 0.1 mm at baseline to 3.6 ± 0.1 mm at day 10.[13] Furthermore, a 2014 follow-up study by Zeglinkski *et al.* illustrated that WT female mice receiving the combination of DOX+TRZ demonstrated a drop in LVEF from 75 ± 3% at baseline to 46 ± 2% at day 10, as demonstrated by echocardiography.[14] Collectively, these basic science studies demonstrate the potent cardiotoxic side effects of DOX and TRZ in both male and female mice.

Our current findings are consistent with the previously validated echocardiographic studies of a DOX+TRZ model of drug-induced cardiomyopathy.[12, 14, 119] In the current study evaluating female mice treated with DOX+TRZ, we demonstrated an increase in LVEDD by 26% and a decrease in LVEF by 41% [120] as compared to baseline. The prophylactic treatment with NACA in DOX+TRZ treated mice significantly attenuated the degree of LV cavity dilatation to only 11% as compared to baseline. Furthermore, NACA also attenuated the decrease in LVEF DOX+TRZ treated mice. The mice administered DOX+TRZ had a drop in LVEF from 73±4% at baseline to 32±2% at day 10, while the group receiving prophylactic NACA in addition to DOX+TRZ, maintained an LVEF of 55±3 % at day 10. Given these echocardiographic findings, we have successfully demonstrated the cardioprotective effects of the novel anti-oxidant NACA in a female murine model of drug-induced cardiomyopathy for the first time.

Previous studies have also evaluated the potential therapeutic effects of other cardioprotective agents. In particular, prior investigations have characterized the potential cardioprotective effects of iron chelating agents, β-blockers, ACE inhibitors, and anti-oxidants including Probucol.[13, 121-124] The clincal use of ACE inhibitors has led to significant improvements in overall morbidity and mortality in cancer patients who develop heart failure.[116-119] Patients who suffer from heart failure, including DOX induced cardiomyopathy are often treated with ACE inhibitors following the development of LV systolic dysfunction.[125] Similarily, β-blockers have also been evaluated for their efficacy in treating heart failure, and are often used following the development of systolic dysfunction.[126] Despite this, to date, there are no known therapies that have been validated as prophylactic treatment for chemotherapy induced cardiotoxicity.

Investigations into the potential role of ACE inhibitors as prophylactic treatment for anthracycline-mediated cardiomyopathy have been established in both the basic science and clinical setting.[68, 127, 128] In animal studies, the prophylactic administration of ACE inhibitors was partially cardioprotective in both the acute and chronic models of anthracycline mediated cardiac dysfunction.[128] In recent clinical studies, combination treatment with ACE inhibitors and β-blockers was postulated to prevent LV systolic dysfunction in patients undergoing chemotherapy.[129] Additionally, the use of anti-oxidants such as Probucol has also seen to be cardio-protective in the setting of chemotherapy induced cardiac dysfunction. A major side effect to the use of Probucol as a prophylactic cardioprotective agent is its pro-arrhythmic effects, and gastrointestinal

discomfort.[130] Despite these promising findings from a multitude of studies, no medications are currently approved for the prevention of chemotherapy-induced cardiotoxicity. Given this, our findings have shown the potential role for the novel anti-oxidant NACA in the setting of chemotherapy-induced cardiomyopathy. NACA does not have any known side effects thereby making it a suitable prophylactic agent in DOX+TRZ mediated cardiomyopathy. [107]

6.3 Histology

Doxorubicin induced cardiotoxicty is characterized by a loss of cellular integrity, as validated by both animal and human studies.[131, 132] Electron microscopy analyses by Siveski-Iliskovic *et al*. illustrated the histological manifestation of cardiomyopathy in mice treated with a cumulative dose of 15 mg/kg of DOX over a two-week period.[131] They demonstrated significant mitochondrial swelling, vacuolization of the cytoplasm, formation of lysosomal bodies, and dilatation of the sarcotubular system.[131] Further investigation at higher magnification revealed loss or distortion of the cristae within the mitochondria. Additional studies by our group have collectively confirmed the microscopic evidence of extensive myofibrillar degradation and cellular vacuolization in mice treated with DOX.[12-14] All three studies also reported that mice treated with DOX+TRZ had significantly more myocardial damage than those mice receiving mono therapy with DOX alone.[12, 13]

Similarly, our current findings also demonstrate that treatment with DOX or DOX+TRZ in female mice results in significant histological damage to the cardiomyocytes. In WT mice treated with DOX+TRZ, significant myofibrillar degradation, vacuolization, loss of sarcomere integrity, and sarcoplasmic reticulum

dilation was observed. All of these histological manifestations were attenuated with the prophylactic administration of NACA in DOX+TRZ treated mice. This novel finding suggests that NACA is cardio-protective in this drug-induced cardiomyopathy.

Translating these basic science findings into the clinical context can be accomplished by examination of invasive myocardial biopsy tissue. Clinical biopsies from the right ventricle (RV) have demonstrated that treatment with DOX causes loss of myofibrils, vacuolization of the cytoplasm, and distention of the sarcoplasmic reticulum.[132] Bristow *et al.* investigated the endomyocardial changes associated with 545 mg/kg of DOX (cumulative dose) in 33 patients that presented with symptoms of heart failure. The study confirmed that the DOX related changes in the biopsy samples were congruent with previously mentioned observations.[132] Moreover, clinical investigations into cardiac remodeling in TRZ treated patients has also been evaluated. Ewer *et al.* evaluated TRZ-mediated cardiac remodeling in RV biopsy samples from 9 women who received TRZ monotherapy.[133] The main findings from the study showed that none of the women displayed any adverse cardiac remodeling from TRZ treatment, suggesting that anthracycline therapy is the driving force to adverse cardiac effects, those of which are potentiated with conjunct TRZ therapy.[133] Given this observation, the introduction of novel antioxidants such as NACA as prophylactic cardioprotective agents for patients receiving DOX+TRZ therapy remains a promising therapeutic approach.

6.4 Cytoarchitecture

The mechanism of DOX induced cellular damage has been attributed to increases in OS, which lead to damage in key cytoskeletal and other structural elements including desmin, dystrophin, myosin, and connexin-43.[134, 135] A previous study by Campos *et al.* explored the deleterious effects of DOX at cumulative doses up to 15mg/kg in male rats. The main findings of this study showed that myocardium exposed to a cumulative dose of 15mg/kg of DOX over 14 days displayed diffuse foci of disrupted actin, myosin, and dystrophin, reflecting a disrupted sarcomeric structure.[134] The study reported that at 14 days after DOX treatment, there was a significant decrease of dystrophin, a protein normally responsible for connecting the extracellular matrix and the cytoskeleton to cardiomyocyte contraction.[136] In addition, multiple studies have also shown that in failing human hearts, the intermyofibirillar pattern of dystrophin seems to increase initially, potentially functioning as an acute recovery strategy in which cardiomyocytes are trying to improve myofibrillar stability.[137, 138]

Contrary to these previous studies, our findings demonstrated no significant changes in the amounts of desmin, dystrophin, myosin, and connexin-43 following DOX or DOX+TRZ therapy at day 10. It can be speculated from our findings that day 10 may have been too early to detect decreased levels of cytoskeletal proteins due to DOX+TRZ mediated cardiotoxicty. Given the significant drop in LVEF in the acute model of DOX+TRZ mediated cardiotoxicity, these proteins may be rendered dysfunctional but yet remain localized within the myofibril, thereby explaining our

findings Further investigation is required to determine the potential mitigating effects of NACA in DOX+TRZ mediated cytoskeletal damage in a chronic model.

6.5 OS: Superoxides and Oxidized Phospholipids

A potential mechanism for the inherent cardiotoxicity associated with DOX treatment includes increased formation of OS. Previous studies have shown that isolated cardiac mitochondria are known to form complexes with DOX.[139] Specifically, DOX associates with cardiolipin found within the inner mitochondrial membrane of cardiomyocytes, where it is subject to reduction by NADH dehydrogenase from the respiratory chain, resulting in the formation of a semiquinone free radical.[140] This semiquinone radical is oxidized back to its parental compound, thereby transferring an electron to molecular oxygen, thus generating superoxide radicals that are known to render cardiomyocytes non-functional.[141] Mukhopadhyay *et al.* conducted a study in 2009 that demonstrated the effect of DOX on generation of superoxides. The results showed a 6-fold increase in superoxide formation by day 5 in hearts of male mice treated with DOX.[141] Our findings were comparable in a female model of DOX induced cardiomyopathy. Mice administered DOX had a 3-fold increase in superoxide production by 72 hours post treatment. This increase was as high as 4-fold in mice receiving the combination treatment with DOX+TRZ. Our study also demonstrated that the prophylactic administration of NACA was able to decrease the level of superoxides formed in both DOX and DOX+TRZ treated mice. This novel finding suggests that NACA is able to protect to cardiomyocytes in an acute (72 hour) murine model of drug-induced cardiomyopathy by reducing the degree of OS.

In addition, it has been reported that ROS can cause detrimental changes in the lipid profiles found in the cellular bilayer of cardiomyocytes. Recent studies have outlined the importance of the emerging role of plasma lipidomics in cardiovascular health.[142, 143] It has been established that the oxidative, and subsequent enzymatic modification of cellular lipids leads to the release of many inflammatory cytokines thereby promoting cardiac disease.[142] The dynamic nature and function of cellular phospholipids is dramatically altered when they are exposed to increased levels of superoxides, ultimately rendering them physiologically damaged and responsible for disease progression.[144] A study by Zeglinski *et al.* explored the effects of DOX+TRZ on the overall lipid profiles in the hearts of mice.[14] The report included the analysis of 82 distinct oxidized phospholipids in each of the experimental groups. The results showed a significant increase in the overall amount of oxidized phospholipids in the hearts of mice treated with DOX+TRZ in comparison to the saline treated animals.[14] These findings confirmed the effects of OS on lipid composition and the involvement of oxidized phospholipids in drug induced cardiomyopathy.

Similarly, our findings also showed significant changes in the lipid profiles of hearts that were subject to DOX+TRZ mediated cardiac dysfunction. Female mice treated with DOX or DOX+TRZ had approximately 3-fold to 4-fold increases in the amount of fragmented oxidized phospholipids as compared to saline treated animals at 72 hours post treatment, respectively. Our findings also showed that NACA was able to attenuate the degree of OS by significantly decreasing the amount of oxidized phospholipids in both groups. Given the severe effects of the oxidation of

phospholipids, the ability for NACA to offer protection to the lipid profile of cells may offer therapeutic insight into mitigating the effects of DOX+TRZ mediated cardiac dysfunction.

6.6 Apoptosis

Programmed cell death, commonly known as apoptosis, has been seen to play a pivotal role in many experimental and clinical studies exploring cardiac dysfunction.[145-148] A previous study by Kumar *et al.* established a chronic *in vivo* model in which rats were administered high doses of DOX over a 2 week period. In this study, DOX treated animals were seen to have developed a significantly high rate of apoptosis by day 4, as confirmed by TUNEL assays.[148] The rate of apoptosis progressed onto more severe levels by the endpoint of the study at day 21.[148] This study correlated an increased rate of apoptosis as an increase in the Bax/Bcl-2 ratio, which is the ratio between pro-apoptotic, and anti-apoptotic proteins. The studies results showed an increase in the expression of BAX in the DOX treated group as compared to saline controls.[148] In addition, the study also measured the amount of the pro-apoptotic protein Caspase-3, which showed its highest expression at day 4 of the study.[147, 148] Similarly, a study by Nielan *et al*. corroborated these findings in an acute murine model of chemotherapy induced cardiac dysfunction. The study showed that wild type mice receiving a one-time dose of DOX went to develop severe cardiac dysfunction, which was associated with an increased Bax/Bcl-X_L ratio.[119] These studies suggest that apoptotic pathways are intimately involved, and in part, responsible for the cell death of cardiac myocytes in animals treated with DOX.

In addition to DOX induced apoptosis, TRZ therapy has also been seen to increase cellular apoptosis. A study conducted by Grazaette *et al.* used the monocolonal antibody TRZ for the HER2 receptor in an *in vitro* model in which the results showed an increase in the ratio between Bcl-X_s and Bcl-X_L.[66] Increases in the amount of the pro-apoptotic Bcl-X_s, and decreases in the amount of the anti-apoptotic Bcl-X_L are indicative of an increased rate of overall apoptosis, leading to eventual mitochondrial dysfunction. Furthermore, the studies results also revealed that TUNEL staining and propidium iodide flow cytometry also revealed increased rates of apoptosis in TRZ treated cardiomyocytes.[66]

Exploring the combined effects of DOX+TRZ, Jassal *et al.* confirmed that the combination treatment with both drugs lead to an increased degree of apoptosis, as compared to monotherapy with either drug alone, in an acute murine model of chemotherapy.[12] The combination treatment in WT male mice showed the highest degree of apoptosis by day 10, as compared to either anti-cancer agent alone.[12] This chemotherapy-induced apoptosis was characterized by in increase in key pro-apoptotic proteins, including PARP, Caspase-3, and the aforementioned BAX/Bcl-X_L ratio. These findings demonstrate that combined therapy with DOX+TRZ potentiates the apoptotic effects as compared to either agent alone. To further corroborate these findings, a recent study by Walker *et al.* in 2011 showed that male mice treated with DOX+TRZ had much more pronounced cardiac dysfunction than those administered either drug alone.[13] The degree of apoptosis in this study was exemplified by the Bax/Bcl-X_L ratio, which was reported to be highest at day 10.[13] In addition, this study also demonstrated the cardioprotective role of Probucol, an

antioxidant, in DOX+TRZ mediated cardiac dysfunction. The findings showed that Probucol was able to offer cardioprotection by showing improved survival, preserved cardiac systolic function, and attenuation of apoptosis. Both of these studies illustrate the effects of DOX+TRZ on the cell death pathways, thereby offering insight into a potential mechanism of damage for this drug-induced cardiomyopathy.

Similarly, our findings showed a significant increase in the Bax/Bcl-X_L ratio and Caspase-3 at the protein level in WT female mice. Consistent with previous studies, DOX therapy alone revealed a significant increase in the expression of Bax and Caspase-3, along with a decreased expression of Bcl-X_L. Both of these findings suggest that the rate of apoptosis was significantly higher in DOX treated mice as compared to saline controls. Moreover, the combined therapy with DOX+TRZ had an even more pronounced increase in these pro-apoptotic proteins; suggesting that the combined therapy induced the highest rate of apoptosis, which is congruent with prior studies. Prophylactic treatment with NACA was seen to cause significant, but moderate decreases in the Bax/Bcl-X_L ratio and Caspase-3 at the protein level for both DOX and DOX+TRZ treated mice. These findings indicate that NACA may be able to offer a protective effect in DOX+TRZ mediated cardiotoxicty by attenuating the degree of apoptosis.

Given our findings, the prophylactic treatment with NACA to DOX or DOX+TRZ treated mice had a very pronounced recovery of LVEF, as seen from our echocardiographic findings. The degree of rescue from our apoptotic studies showed a much more moderate degree of protection from the use of prophylactic

NACA in both the DOX and DOX+TRZ treated mice. These findings imply that there may be other cell death pathways involved in DOX+TRZ mediated cardiac dysfunction. Autophagy is an apoptotic independent pathway, which may be responsible for chemotherapy, induced cardiac dysfunction in our murine model. Under normal physiological conditions, autophagy is a process that removes damaged cellular organelles and acts as a recycling mechanism, which aids in the maintenance of homeostasis.[149] The involvement of autophagy in mice treated with DOX as been previously described by Kobayashi *et al.*[150] The study concluded that the microtubule light chain 3 (LC3-II) is a marker for autophagy, which is seen to increase in DOX treated mice.[150] Additionally, Zhang *et al.* also showed that mice treated with DOX had a significant increase in the level of pro-autophagy marker LC3-II at 24 hours post treatment.[151] These studies substantiate the potential involvement of autophagy in the development of DOX induced cardiac dysfunction. Further investigation is required to determine the role of autophagy in DOX+TRZ mediated cardiotoxicity.

Another cell death pathway involved in DOX mediated cardiotoxicity is necrosis, which is defined as premature rupture of the cellular plasma membrane with subsequent swelling of cytoplasmic organelles.[149] A study by Lim *et al.* revealed that adult rat cardiomyocytes exposed to DOX showed an increase in trypan blue uptake and CK release, both of which are characteristic of necrosis.[92] This study correlated these results to an activation of calpains and showed that inhibition of calpain activity resulted in minimal trypan blue uptake, resulting in attenuated necrosis.[92] Necrosis has been associated with DOX treatment by resulting in

mitochondrial dysfunction, and loss of cell membrane integrity. Furthermore, the induction of necrosis has also been attributed to an increase in OS, which is typical in DOX+TRZ therapy as seen by our superoxide and oxidized phospholipid analyses.[152] A further understanding of the involvement of necrosis in DOX+TRZ mediated cardiac dysfunction is required in order to accurately define the role of this cell death pathway in this cardiomyopathy. Ultimately, DOX+TRZ mediated cardiotoxicty is likely to be a product of the combined effects of apoptosis, autophagy, and necrosis. Further research into the involvement of these three pathways in DOX+TRZ mediated heart failure is warranted.

6.7 Limitations and Future Directions

There are a number of limitations to our study. First, our study only explored chemotherapy-induced cardiac dysfunction in an acute female murine model of DOX+TRZ mediated cardiac dysfunction. In future studies, we will consider the use of chronic dosing studies in order to simulate the clinical setting in which DOX+TRZ are administered over a longer period of time. In subsequent studies, we will also evaluate the level of activated calcium dependent proteases known as Calpains, and explore their role in DOX+TRZ mediated cardiac dysfunction. In addition, the comprehensive characterization of DOX+TRZ mediated cardiotoxicity requires in depth analysis of how these two anti-cancer agents influence alternative cell death pathways, specifically, necrosis and autophagy. Finally, our future studies will also evaluate whether NACA prevents the anti-cancer efficacy of DOX+TRZ in an *in vivo* model of breast cancer, thereby making our findings more easily translatable to the clinical setting.

6.8 Clinical Implications

The application of NACA as a cardioprotective agent against DOX+TRZ mediated cardiac dysfunction is a novel and clinically applicable finding. Although dexrazoxane, ACEI, and β-blockers may be useful in the setting of DOX induced cardiotoxicity, their efficacy in DOX+TRZ mediated cardiac dysfunction remains to be explored. Prubocol is a pharmacological agent that has been proposed as a cardioprotective agent against DOX+TRZ induced carditoxicity, but its clinical use in this setting is being limited due to its side effects. NACA is a novel anti-oxidant with no known side effects; thereby making it a promising cardioprotective agent in DOX+TRZ mediated cardiac damage. Further clinical investigation into the potential role of NACA as a prophylactic agent is warranted.

Chapter 7: Summary and Conclusion

7.1 Summary of Findings

To summarize our current studies' main findings:

1. Mice receiving DOX had their LVEF decrease from 73±4% to 43±2% at day 10. In mice receiving DOX+TRZ, LVEF decreased from 72±3% to 32±2% at day 10. Prophylactic administration of NACA to mice receiving DOX or DOX+TRZ was cardio-protective with an LVEF of 62±3% and 55±3% at day 10, respectively.
2. Histological analyses revealed DOX+TRZ treated mice had significant myofibrillar disarray as seen through electron microscopy, which was also attenuated by prophylactic NACA administration. Additionally, there was a 3-fold and 4-fold increase in superoxide production in mice treated with DOX or DOX+TRZ, respectively, which was also attenuated by the prophylactic administration of NACA.
3. Similarly, although the degree of oxidized phospholipids was increased in mice receiving DOX or DOX+TRZ, the prophylactic administration of NACA attenuated the degree of OS in both groups.
4. Finally, there was a 1.5-fold and 2 fold increase in the Bax/Bcl-xL ratio in hearts of mice treated with DOX or DOX+TRZ, respectively. Prophylactic administration of NACA attenuated the amounts of these pro-apoptotic proteins thereby suggesting a decreased induction of apoptotic pathways.

7.2 Conclusion

We are the first group to describe the effects of prophylactic therapy with the antioxidant NACA in DOX+TRZ mediated cardiac dysfunction. Our novel study demonstrates that NACA preserves systolic function and attenuates the cardiotoxic effects of DOX+TRZ. Future studies evaluating the cardioprotective effects of NACA in the clinical setting of breast cancer are warranted.

References

1. Carlos L. Arteaga MXS, C. Kent Osborne, Edith A. Perez, Fabio Puglisi & Luca Gianni. Treatment of HER2-positive breast cancer: current status and future perspectives. *Nature Reviews Clinical Oncology*. 2012;9:16-32.

2. Canadian Cancer Society's Advisory Committee on Cancer Statistics. *Canadian Cancer Society* 2014.

3. Bigenwald RZ, Warner E, Gunasekara A, Hill KA, Causer PA, Messner SJ, Eisen A, Plewes DB, Narod SA, Zhang L and Yaffe MJ. Is mammography adequate for screening women with inherited BRCA mutations and low breast density? *Cancer Epidemiol Biomarkers Prev*. 2008;17:706-11.

4. Kolb TM, Lichy J and Newhouse JH. Comparison of the performance of screening mammography, physical examination, and breast US and evaluation of factors that influence them: an analysis of 27,825 patient evaluations. *Radiology*. 2002;225:165-75.

5. Warner E, Messersmith H, Causer P, Eisen A, Shumak R and Plewes D. Systematic review: using magnetic resonance imaging to screen women at high risk for breast cancer. *Ann Intern Med*. 2008;148:671-9.

6. Warner E, Plewes DB, Hill KA, Causer PA, Zubovits JT, Jong RA, Cutrara MR, DeBoer G, Yaffe MJ, Messner SJ, Meschino WS, Piron CA and Narod SA. Surveillance of BRCA1 and BRCA2 mutation carriers with magnetic resonance imaging, ultrasound, mammography, and clinical breast examination. *JAMA*. 2004;292:1317-25.

7. Capala J and Bouchelouche K. Molecular imaging of HER2-positive breast cancer: a step toward an individualized 'image and treat' strategy. *Curr Opin Oncol*. 2010;22:559-66.

8. McPherson K, Steel CM and Dixon JM. ABC of breast diseases. Breast cancer-epidemiology, risk factors, and genetics. *BMJ*. 2000;321:624-8.

9. Taghian AG and Powell SN. The role of radiation therapy for primary breast cancer. *Surg Clin North Am*. 1999;79:1091-115.

10. Ragaz J, Olivotto IA, Spinelli JJ, Phillips N, Jackson SM, Wilson KS, Knowling MA, Coppin CM, Weir L, Gelmon K, Le N, Durand R, Coldman AJ and Manji M. Locoregional radiation therapy in patients with high-risk breast cancer receiving adjuvant chemotherapy: 20-year results of the British Columbia randomized trial. *J Natl Cancer Inst*. 2005;97:116-26.

11. Olver IN. Trastuzumab as the lead monoclonal antibody in advanced breast cancer: choosing which patient and when. *Future Oncol*. 2008;4:125-31.

12. Jassal DS, Han SY, Hans C, Sharma A, Fang T, Ahmadie R, Lytwyn M, Walker JR, Bhalla RS, Czarnecki A, Moussa T and Singal PK. Utility of tissue Doppler and strain rate imaging in the early detection of trastuzumab and anthracycline mediated cardiomyopathy. *J Am Soc Echocardiogr*. 2009;22:418-24.

13. Walker JR, Sharma A, Lytwyn M, Bohonis S, Thliveris J, Singal PK and Jassal DS. The cardioprotective role of probucol against anthracycline and trastuzumab-mediated cardiotoxicity. *J Am Soc Echocardiogr*. 2011;24:699-705.

14. Zeglinski M, Premecz S, Lerner J, Wtorek P, Dasilva M, Hasanally D, Chaudhary R, Sharma A, Thliveris J, Ravandi A, Singal PK and Jassal DS. Congenital

absence of nitric oxide synthase 3 potentiates cardiac dysfunction and reduces survival in doxorubicin- and trastuzumab-mediated cardiomyopathy. *Can J Cardiol*. 2014;30:359-67.

15. Unverferth DV, Jagadeesh JM, Unverferth BJ, Magorien RD, Leier CV and Balcerzak SP. Attempt to prevent doxorubicin-induced acute human myocardial morphologic damage with acetylcysteine. *J Natl Cancer Inst*. 1983;71:917-20.

16. Rabbani A, Finn RM and Ausio J. The anthracycline antibiotics: antitumor drugs that alter chromatin structure. *Bioessays*. 2005;27:50-6.

17. Weiss RB, Sarosy G, Clagett-Carr K, Russo M and Leyland-Jones B. Anthracycline analogs: the past, present, and future. *Cancer Chemother Pharmacol*. 1986;18:185-97.

18. Cassinelli G, Ballabio M, Arcamone F, Casazza AM and Podesta A. New anthracycline glycosides obtained by the nitrous acid deamination of daunorubicin, doxorubicin and their configurational analogues. *J Antibiot (Tokyo)*. 1985;38:856-67.

19. Singal PK and Iliskovic N. Doxorubicin-induced cardiomyopathy. *N Engl J Med*. 1998;339:900-5.

20. Minotti G, Menna P, Salvatorelli E, Cairo G and Gianni L. Anthracyclines: molecular advances and pharmacologic developments in antitumor activity and cardiotoxicity. *Pharmacol Rev*. 2004;56:185-229.

21. Singal PK, Iliskovic N, Li T and Kumar D. Adriamycin cardiomyopathy: pathophysiology and prevention. *FASEB J*. 1997;11:931-6.

22. Gewirtz DA. A critical evaluation of the mechanisms of action proposed for the antitumor effects of the anthracycline antibiotics adriamycin and daunorubicin. *Biochem Pharmacol*. 1999;57:727-41.

23. Muggia FM and Green MD. New anthracycline antitumor antibiotics. *Crit Rev Oncol Hematol*. 1991;11:43-64.

24. Pang B, Qiao X, Janssen L, Velds A, Groothuis T, Kerkhoven R, Nieuwland M, Ovaa H, Rottenberg S, van Tellingen O, Janssen J, Huijgens P, Zwart W and Neefjes J. Drug-induced histone eviction from open chromatin contributes to the chemotherapeutic effects of doxorubicin. *Nat Commun*. 2013;4:1908.

25. Takemura G and Fujiwara H. Doxorubicin-induced cardiomyopathy from the cardiotoxic mechanisms to management. *Prog Cardiovasc Dis*. 2007;49:330-52.

26. Peng X, Chen B, Lim CC and Sawyer DB. The cardiotoxicology of anthracycline chemotherapeutics: translating molecular mechanism into preventative medicine. *Mol Interv*. 2005;5:163-71.

27. Fisher LM, Austin CA, Hopewell R, Margerrison EE, Oram M, Patel S, Plummer K, Sng JH and Sreedharan S. DNA supercoiling and relaxation by ATP-dependent DNA topoisomerases. *Philos Trans R Soc Lond B Biol Sci*. 1992;336:83-91.

28. Scheltema JM, Romijn JC, van Steenbrugge GJ, Beck WT, Schroder FH and Mickisch GH. Decreased levels of topoisomerase II alpha in human renal cell carcinoma lines resistant to etoposide. *J Cancer Res Clin Oncol*. 1997;123:546-54.

29. Gruber BM, Anuszewska EL, Roman I, Gozdzik A, Priebe W and Fokt I. Topoisomerase II alpha expression and cytotoxicity of anthracyclines in human neoplastic cells. *Acta Pol Pharm*. 2006;63:15-8.

30. Binaschi M, Capranico G, Dal Bo L and Zunino F. Relationship between lethal effects and topoisomerase II-mediated double-stranded DNA breaks produced by anthracyclines with different sequence specificity. *Mol Pharmacol*. 1997;51:1053-9.

31. Ludke AR, Al-Shudiefat AA, Dhingra S, Jassal DS and Singal PK. A concise description of cardioprotective strategies in doxorubicin-induced cardiotoxicity. *Can J Physiol Pharmacol*. 2009;87:756-63.

32. Chen B, Peng X, Pentassuglia L, Lim CC and Sawyer DB. Molecular and cellular mechanisms of anthracycline cardiotoxicity. *Cardiovasc Toxicol*. 2007;7:114-21.

33. Lefrak EA, Pitha J, Rosenheim S and Gottlieb JA. A clinicopathologic analysis of adriamycin cardiotoxicity. *Cancer*. 1973;32:302-14.

34. Barry E, Alvarez JA, Scully RE, Miller TL and Lipshultz SE. Anthracycline-induced cardiotoxicity: course, pathophysiology, prevention and management. *Expert Opin Pharmacother*. 2007;8:1039-58.

35. Hackel PO, Zwick E, Prenzel N and Ullrich A. Epidermal growth factor receptors: critical mediators of multiple receptor pathways. *Curr Opin Cell Biol*. 1999;11:184-9.

36. Yarden Y and Sliwkowski MX. Untangling the ErbB signalling network. *Nat Rev Mol Cell Biol*. 2001;2:127-37.

37. Worthylake R and Wiley HS. Structural aspects of the epidermal growth factor receptor required for transmodulation of erbB-2/neu. *J Biol Chem*. 1997;272:8594-601.

38. Cho HS, Mason K, Ramyar KX, Stanley AM, Gabelli SB, Denney DW, Jr. and Leahy DJ. Structure of the extracellular region of HER2 alone and in complex with the Herceptin Fab. *Nature*. 2003;421:756-60.

39. Moghal N and Sternberg PW. Multiple positive and negative regulators of signaling by the EGF-receptor. *Curr Opin Cell Biol*. 1999;11:190-6.

40. Graus-Porta D, Beerli RR, Daly JM and Hynes NE. ErbB-2, the preferred heterodimerization partner of all ErbB receptors, is a mediator of lateral signaling. *EMBO J*. 1997;16:1647-55.

41. Negro A, Brar BK and Lee KF. Essential roles of Her2/erbB2 in cardiac development and function. *Recent Prog Horm Res*. 2004;59:1-12.

42. Pegram M and Slamon D. Biological rationale for HER2/neu (c-erbB2) as a target for monoclonal antibody therapy. *Semin Oncol*. 2000;27:13-9.

43. Plosker GL and Keam SJ. Spotlight on Trastuzumab in the management of HER2-positive metastatic and early-stage breast cancer. *BioDrugs*. 2006;20:259-62.

44. Suter TM, Cook-Bruns N and Barton C. Cardiotoxicity associated with trastuzumab (Herceptin) therapy in the treatment of metastatic breast cancer. *Breast*. 2004;13:173-83.

45. Suter TM, Procter M, van Veldhuisen DJ, Muscholl M, Bergh J, Carlomagno C, Perren T, Passalacqua R, Bighin C, Klijn JG, Ageev FT, Hitre E, Groetz J, Iwata H, Knap M, Gnant M, Muehlbauer S, Spence A, Gelber RD and Piccart-Gebhart MJ. Trastuzumab-associated cardiac adverse effects in the herceptin adjuvant trial. *J Clin Oncol*. 2007;25:3859-65.

46. Press MF, Slamon DJ, Flom KJ, Park J, Zhou JY and Bernstein L. Evaluation of HER-2/neu gene amplification and overexpression: comparison of frequently used assay methods in a molecularly characterized cohort of breast cancer specimens. *J Clin Oncol*. 2002;20:3095-105.

47. Hicks DG and Tubbs RR. Assessment of the HER2 status in breast cancer by fluorescence in situ hybridization: a technical review with interpretive guidelines. *Hum Pathol*. 2005;36:250-61.

48. Bilous M, Ades C, Armes J, Bishop J, Brown R, Cooke B, Cummings M, Farshid G, Field A, Morey A, McKenzie P, Raymond W, Robbins P and Tan L. Predicting the HER2 status of breast cancer from basic histopathology data: an analysis of 1500 breast cancers as part of the HER2000 International Study. *Breast*. 2003;12:92-8.

49. Plosker GL and Keam SJ. Trastuzumab: a review of its use in the management of HER2-positive metastatic and early-stage breast cancer. *Drugs*. 2006;66:449-75.

50. Klapper LN, Kirschbaum MH, Sela M and Yarden Y. Biochemical and clinical implications of the ErbB/HER signaling network of growth factor receptors. *Adv Cancer Res*. 2000;77:25-79.

51. Sliwkowski MX, Lofgren JA, Lewis GD, Hotaling TE, Fendly BM and Fox JA. Nonclinical studies addressing the mechanism of action of trastuzumab (Herceptin). *Semin Oncol*. 1999;26:60-70.

52. Slamon DJ, Leyland-Jones B, Shak S, Fuchs H, Paton V, Bajamonde A, Fleming T, Eiermann W, Wolter J, Pegram M, Baselga J and Norton L. Use of chemotherapy plus a monoclonal antibody against HER2 for metastatic breast cancer that overexpresses HER2. *N Engl J Med*. 2001;344:783-92.

53. Romond EH, Perez EA, Bryant J, Suman VJ, Geyer CE, Jr., Davidson NE, Tan-Chiu E, Martino S, Paik S, Kaufman PA, Swain SM, Pisansky TM, Fehrenbacher L, Kutteh LA, Vogel VG, Visscher DW, Yothers G, Jenkins RB, Brown AM, Dakhil SR, Mamounas EP, Lingle WL, Klein PM, Ingle JN and Wolmark N. Trastuzumab plus adjuvant chemotherapy for operable HER2-positive breast cancer. *N Engl J Med*. 2005;353:1673-84.

54. Hudis CA. Trastuzumab--mechanism of action and use in clinical practice. *N Engl J Med*. 2007;357:39-51.

55. Baselga J, Carbonell X, Castaneda-Soto NJ, Clemens M, Green M, Harvey V, Morales S, Barton C and Ghahramani P. Phase II study of efficacy, safety, and pharmacokinetics of trastuzumab monotherapy administered on a 3-weekly schedule. *J Clin Oncol*. 2005;23:2162-71.

56. Piccart-Gebhart MJ, Procter M, Leyland-Jones B, Goldhirsch A, Untch M, Smith I, Gianni L, Baselga J, Bell R, Jackisch C, Cameron D, Dowsett M, Barrios CH, Steger G, Huang CS, Andersson M, Inbar M, Lichinitser M, Lang I, Nitz U, Iwata H, Thomssen C, Lohrisch C, Suter TM, Ruschoff J, Suto T, Greatorex V, Ward C, Straehle C, McFadden E, Dolci MS, Gelber RD and Herceptin Adjuvant Trial Study T. Trastuzumab after adjuvant chemotherapy in HER2-positive breast cancer. *N Engl J Med*. 2005;353:1659-72.

57. Gianni L, Dafni U, Gelber RD, Azambuja E, Muehlbauer S, Goldhirsch A, Untch M, Smith I, Baselga J, Jackisch C, Cameron D, Mano M, Pedrini JL, Veronesi A, Mendiola C, Pluzanska A, Semiglazov V, Vrdoljak E, Eckart MJ, Shen Z, Skiadopoulos G, Procter M, Pritchard KI, Piccart-Gebhart MJ, Bell R and Herceptin Adjuvant Trial

Study T. Treatment with trastuzumab for 1 year after adjuvant chemotherapy in patients with HER2-positive early breast cancer: a 4-year follow-up of a randomised controlled trial. *Lancet Oncol*. 2011;12:236-44.

58. Iles L, Pfluger H, Phrommintikul A, Cherayath J, Aksit P, Gupta SN, Kaye DM and Taylor AJ. Evaluation of diffuse myocardial fibrosis in heart failure with cardiac magnetic resonance contrast-enhanced T1 mapping. *J Am Coll Cardiol*. 2008;52:1574-80.

59. Perez EA, Suman VJ, Davidson NE, Sledge GW, Kaufman PA, Hudis CA, Martino S, Gralow JR, Dakhil SR, Ingle JN, Winer EP, Gelmon KA, Gersh BJ, Jaffe AS and Rodeheffer RJ. Cardiac safety analysis of doxorubicin and cyclophosphamide followed by paclitaxel with or without trastuzumab in the North Central Cancer Treatment Group N9831 adjuvant breast cancer trial. *J Clin Oncol*. 2008;26:1231-8.

60. Baselga J, Perez EA, Pienkowski T and Bell R. Adjuvant trastuzumab: a milestone in the treatment of HER-2-positive early breast cancer. *Oncologist*. 2006;11 Suppl 1:4-12.

61. Seidman A, Hudis C, Pierri MK, Shak S, Paton V, Ashby M, Murphy M, Stewart SJ and Keefe D. Cardiac dysfunction in the trastuzumab clinical trials experience. *J Clin Oncol*. 2002;20:1215-21.

62. NewYorkHeartAssociation. Nomenclature and criteria for diagnosis of diseases of the heart and great vessels. 1994:253-256.

63. Wadhwa D, Fallah-Rad N, Grenier D, Krahn M, Fang T, Ahmadie R, Walker JR, Lister D, Arora RC, Barac I, Morris A and Jassal DS. Trastuzumab mediated

cardiotoxicity in the setting of adjuvant chemotherapy for breast cancer: a retrospective study. *Breast Cancer Res Treat*. 2009;117:357-64.

64. Guarneri V, Lenihan DJ, Valero V, Durand JB, Broglio K, Hess KR, Michaud LB, Gonzalez-Angulo AM, Hortobagyi GN and Esteva FJ. Long-term cardiac tolerability of trastuzumab in metastatic breast cancer: the M.D. Anderson Cancer Center experience. *J Clin Oncol*. 2006;24:4107-15.

65. Gross A, McDonnell JM and Korsmeyer SJ. BCL-2 family members and the mitochondria in apoptosis. *Genes Dev*. 1999;13:1899-911.

66. Grazette LP, Boecker W, Matsui T, Semigran M, Force TL, Hajjar RJ and Rosenzweig A. Inhibition of ErbB2 causes mitochondrial dysfunction in cardiomyocytes: implications for herceptin-induced cardiomyopathy. *J Am Coll Cardiol*. 2004;44:2231-8.

67. Gordon LI, Burke MA, Singh AT, Prachand S, Lieberman ED, Sun L, Naik TJ, Prasad SV and Ardehali H. Blockade of the erbB2 receptor induces cardiomyocyte death through mitochondrial and reactive oxygen species-dependent pathways. *J Biol Chem*. 2009;284:2080-7.

68. Cardinale D, Colombo A, Sandri MT, Lamantia G, Colombo N, Civelli M, Martinelli G, Veglia F, Fiorentini C and Cipolla CM. Prevention of high-dose chemotherapy-induced cardiotoxicity in high-risk patients by angiotensin-converting enzyme inhibition. *Circulation*. 2006;114:2474-81.

69. Nakagami H, Takemoto M and Liao JK. NADPH oxidase-derived superoxide anion mediates angiotensin II-induced cardiac hypertrophy. *J Mol Cell Cardiol*. 2003;35:851-9.

70. Pentassuglia L and Sawyer DB. The role of Neuregulin-1beta/ErbB signaling in the heart. *Exp Cell Res*. 2009;315:627-37.

71. Kuramochi Y, Guo X and Sawyer DB. Neuregulin activates erbB2-dependent src/FAK signaling and cytoskeletal remodeling in isolated adult rat cardiac myocytes. *J Mol Cell Cardiol*. 2006;41:228-35.

72. Crone SA, Zhao YY, Fan L, Gu Y, Minamisawa S, Liu Y, Peterson KL, Chen J, Kahn R, Condorelli G, Ross J, Jr., Chien KR and Lee KF. ErbB2 is essential in the prevention of dilated cardiomyopathy. *Nat Med*. 2002;8:459-65.

73. Singal PK, Khaper N, Palace V and Kumar D. The role of oxidative stress in the genesis of heart disease. *Cardiovasc Res*. 1998;40:426-32.

74. Kirshenbaum LA, Thomas TP, Randhawa AK and Singal PK. Time-course of cardiac myocyte injury due to oxidative stress. *Mol Cell Biochem*. 1992;111:25-31.

75. Singal PK, Petkau A, Gerrard JM, Hrushovetz S and Foerster J. Free radicals in health and disease. *Mol Cell Biochem*. 1988;84:121-2.

76. Pearson G, Robinson F, Beers Gibson T, Xu BE, Karandikar M, Berman K and Cobb MH. Mitogen-activated protein (MAP) kinase pathways: regulation and physiological functions. *Endocr Rev*. 2001;22:153-83.

77. Lou H, Kaur K, Sharma AK and Singal PK. Adriamycin-induced oxidative stress, activation of MAP kinases and apoptosis in isolated cardiomyocytes. *Pathophysiology*. 2006;13:103-9.

78. Carnero A, Blanco-Aparicio C, Renner O, Link W and Leal JF. The PTEN/PI3K/AKT signalling pathway in cancer, therapeutic implications. *Curr Cancer Drug Targets*. 2008;8:187-98.

79. Souchelnytskyi S, Ronnstrand L, Heldin CH and ten Dijke P. Phosphorylation of Smad signaling proteins by receptor serine/threonine kinases. *Methods Mol Biol*. 2001;124:107-20.

80. Zhao W, Zhao T, Chen Y, Ahokas RA and Sun Y. Oxidative stress mediates cardiac fibrosis by enhancing transforming growth factor-beta1 in hypertensive rats. *Mol Cell Biochem*. 2008;317:43-50.

81. Tomasek JJ, Gabbiani G, Hinz B, Chaponnier C and Brown RA. Myofibroblasts and mechano-regulation of connective tissue remodelling. *Nat Rev Mol Cell Biol*. 2002;3:349-63.

82. Massague J. TGF-beta signal transduction. *Annu Rev Biochem*. 1998;67:753-91.

83. Saadane N, Alpert L and Chalifour LE. Expression of immediate early genes, GATA-4, and Nkx-2.5 in adrenergic-induced cardiac hypertrophy and during regression in adult mice. *Br J Pharmacol*. 1999;127:1165-76.

84. Molkentin JD, Kalvakolanu DV and Markham BE. Transcription factor GATA-4 regulates cardiac muscle-specific expression of the alpha-myosin heavy-chain gene. *Mol Cell Biol*. 1994;14:4947-57.

85. Murphy AM, Thompson WR, Peng LF and Jones L, 2nd. Regulation of the rat cardiac troponin I gene by the transcription factor GATA-4. *Biochem J*. 1997;322 (Pt 2):393-401.

86. Aries A, Paradis P, Lefebvre C, Schwartz RJ and Nemer M. Essential role of GATA-4 in cell survival and drug-induced cardiotoxicity. *Proc Natl Acad Sci U S A*. 2004;101:6975-80.

87. Kim Y, Ma AG, Kitta K, Fitch SN, Ikeda T, Ihara Y, Simon AR, Evans T and Suzuki YJ. Anthracycline-induced suppression of GATA-4 transcription factor: implication in the regulation of cardiac myocyte apoptosis. *Mol Pharmacol*. 2003;63:368-77.

88. Arai M, Yoguchi A, Takizawa T, Yokoyama T, Kanda T, Kurabayashi M and Nagai R. Mechanism of doxorubicin-induced inhibition of sarcoplasmic reticulum Ca(2+)-ATPase gene transcription. *Circ Res*. 2000;86:8-14.

89. Emanuelov AK, Shainberg A, Chepurko Y, Kaplan D, Sagie A, Porat E, Arad M and Hochhauser E. Adenosine A3 receptor-mediated cardioprotection against doxorubicin-induced mitochondrial damage. *Biochem Pharmacol*. 2010;79:180-7.

90. Matsumura Y, Saeki E, Inoue M, Hori M, Kamada T and Kusuoka H. Inhomogeneous disappearance of myofilament-related cytoskeletal proteins in stunned myocardium of guinea pig. *Circ Res*. 1996;79:447-54.

91. Papp Z, van der Velden J and Stienen GJ. Calpain-I induced alterations in the cytoskeletal structure and impaired mechanical properties of single myocytes of rat heart. *Cardiovasc Res*. 2000;45:981-93.

92. Lim CC, Zuppinger C, Guo X, Kuster GM, Helmes M, Eppenberger HM, Suter TM, Liao R and Sawyer DB. Anthracyclines induce calpain-dependent titin proteolysis and necrosis in cardiomyocytes. *J Biol Chem*. 2004;279:8290-9.

93. Palace V, Kumar D, Hill MF, Khaper N and Singal PK. Regional differences in non-enzymatic antioxidants in the heart under control and oxidative stress conditions. *J Mol Cell Cardiol*. 1999;31:193-202.

94. Kaul N, Siveski-Iliskovic N, Hill M, Slezak J and Singal PK. Free radicals and the heart. *J Pharmacol Toxicol Methods*. 1993;30:55-67.

95. Halliwell B and Gutteridge JM. The antioxidants of human extracellular fluids. *Arch Biochem Biophys*. 1990;280:1-8.

96. Pompella A, Visvikis A, Paolicchi A, De Tata V and Casini AF. The changing faces of glutathione, a cellular protagonist. *Biochem Pharmacol*. 2003;66:1499-503.

97. Hayes JD and McLellan LI. Glutathione and glutathione-dependent enzymes represent a co-ordinately regulated defence against oxidative stress. *Free Radic Res*. 1999;31:273-300.

98. Green JL, Heard KJ, Reynolds KM and Albert D. Oral and Intravenous Acetylcysteine for Treatment of Acetaminophen Toxicity: A Systematic Review and Meta-analysis. *West J Emerg Med*. 2013;14:218-26.

99. Tirouvanziam R, Conrad CK, Bottiglieri T, Herzenberg LA, Moss RB and Herzenberg LA. High-dose oral N-acetylcysteine, a glutathione prodrug, modulates inflammation in cystic fibrosis. *Proc Natl Acad Sci U S A*. 2006;103:4628-33.

100. Tepel M, van der Giet M, Schwarzfeld C, Laufer U, Liermann D and Zidek W. Prevention of radiographic-contrast-agent-induced reductions in renal function by acetylcysteine. *N Engl J Med*. 2000;343:180-4.

101. Kupchik YM, Moussawi K, Tang XC, Wang X, Kalivas BC, Kolokithas R, Ogburn KB and Kalivas PW. The effect of N-acetylcysteine in the nucleus accumbens on neurotransmission and relapse to cocaine. *Biol Psychiatry*. 2012;71:978-86.

102. Holdiness MR. Clinical pharmacokinetics of N-acetylcysteine. *Clin Pharmacokinet*. 1991;20:123-34.

103. Cotgreave IA. N-acetylcysteine: pharmacological considerations and experimental and clinical applications. *Adv Pharmacol*. 1997;38:205-27.

104. Banerjee A, Zhang X, Manda KR, Banks WA and Ercal N. HIV proteins (gp120 and Tat) and methamphetamine in oxidative stress-induced damage in the brain: potential role of the thiol antioxidant N-acetylcysteine amide. *Free Radic Biol Med*. 2010;48:1388-98.

105. Grinberg L, Fibach E, Amer J and Atlas D. N-acetylcysteine amide, a novel cell-permeating thiol, restores cellular glutathione and protects human red blood cells from oxidative stress. *Free Radic Biol Med*. 2005;38:136-45.

106. Offen D, Gilgun-Sherki Y, Barhum Y, Benhar M, Grinberg L, Reich R, Melamed E and Atlas D. A low molecular weight copper chelator crosses the blood-brain barrier and attenuates experimental autoimmune encephalomyelitis. *J Neurochem*. 2004;89:1241-51.

107. Shi R, Huang CC, Aronstam RS, Ercal N, Martin A and Huang YW. N-acetylcysteine amide decreases oxidative stress but not cell death induced by doxorubicin in H9c2 cardiomyocytes. *BMC Pharmacol*. 2009;9:7.

108. Sunitha K, Hemshekhar M, Thushara RM, Santhosh MS, Yariswamy M, Kemparaju K and Girish KS. N-Acetylcysteine amide: a derivative to fulfill the promises of N-Acetylcysteine. *Free Radic Res*. 2013;47:357-67.

109. Akolkar G, Bhullar N, Bews H, Shaikh B, Premecz S, Bordun KA, Cheung DY, Goyal V, Sharma AK, Garber P, Singal PK and Jassal DS. The role of renin angiotensin system antagonists in the prevention of doxorubicin and trastuzumab induced cardiotoxicity. *Cardiovasc Ultrasound*. 2015;13:18.

110. Ahmadie R, Santiago JJ, Walker J, Fang T, Le K, Zhao Z, Azordegan N, Bage S, Lytwyn M, Rattan S, Dixon IM, Kardami E, Moghadasian MH and Jassal DS. A high-lipid diet potentiates left ventricular dysfunction in nitric oxide synthase 3-deficient mice after chronic pressure overload. *J Nutr*. 2010;140:1438-44.

111. Sebag IA, Handschumacher MD, Ichinose F, Morgan JG, Hataishi R, Rodrigues AC, Guerrero JL, Steudel W, Raher MJ, Halpern EF, Derumeaux G, Bloch KD, Picard MH and Scherrer-Crosbie M. Quantitative assessment of regional myocardial function in mice by tissue Doppler imaging: comparison with hemodynamics and sonomicrometry. *Circulation*. 2005;111:2611-6.

112. Luft JH. Improvements in epoxy resin embedding methods. *J Biophys Biochem Cytol*. 1961;9:409-14.

113. Gruber F, Bicker W, Oskolkova OV, Tschachler E and Bochkov VN. A simplified procedure for semi-targeted lipidomic analysis of oxidized phosphatidylcholines induced by UVA irradiation. *J Lipid Res*. 2012;53:1232-42.

114. Livak KJ and Schmittgen TD. Analysis of relative gene expression data using real-time quantitative PCR and the 2(-Delta Delta C(T)) Method. *Methods*. 2001;25:402-8.

115. Mandal S, Curtis L, Pind M, Murphy LC and Watson PH. S100A7 (psoriasin) influences immune response genes in human breast cancer. *Exp Cell Res*. 2007;313:3016-25.

116. Zeglinski M, Ludke A, Jassal DS and Singal PK. Trastuzumab-induced cardiac dysfunction: A 'dual-hit'. *Exp Clin Cardiol*. 2011;16:70-4.

117. Saeed MF, Premecz S, Goyal V, Singal PK and Jassal DS. Catching broken hearts: pre-clinical detection of doxorubicin and trastuzumab mediated cardiac dysfunction in the breast cancer setting. *Can J Physiol Pharmacol*. 2014;92:546-50.

118. Walker J, Bhullar N, Fallah-Rad N, Lytwyn M, Golian M, Fang T, Summers AR, Singal PK, Barac I, Kirkpatrick ID and Jassal DS. Role of three-dimensional echocardiography in breast cancer: comparison with two-dimensional echocardiography, multiple-gated acquisition scans, and cardiac magnetic resonance imaging. *J Clin Oncol*. 2010;28:3429-36.

119. Neilan TG, Blake SL, Ichinose F, Raher MJ, Buys ES, Jassal DS, Furutani E, Perez-Sanz TM, Graveline A, Janssens SP, Picard MH, Scherrer-Crosbie M and Bloch KD. Disruption of nitric oxide synthase 3 protects against the cardiac injury, dysfunction, and mortality induced by doxorubicin. *Circulation*. 2007;116:506-14.

120. Richardson P, McKenna W, Bristow M, Maisch B, Mautner B, O'Connell J, Olsen E, Thiene G, Goodwin J, Gyarfas I, Martin I and Nordet P. Report of the 1995 World Health Organization/International Society and Federation of Cardiology Task Force on the Definition and Classification of cardiomyopathies. *Circulation*. 1996;93:841-2.

121. Hershko C, Pinson A and Link G. Prevention of anthracycline cardiotoxicity by iron chelation. *Acta Haematol*. 1996;95:87-92.

122. Pfeffer MA, Braunwald E, Moye LA, Basta L, Brown EJ, Jr., Cuddy TE, Davis BR, Geltman EM, Goldman S, Flaker GC and et al. Effect of captopril on mortality and morbidity in patients with left ventricular dysfunction after myocardial infarction.

Results of the survival and ventricular enlargement trial. The SAVE Investigators. *N Engl J Med*. 1992;327:669-77.

123. Yusuf S, Sleight P, Pogue J, Bosch J, Davies R and Dagenais G. Effects of an angiotensin-converting-enzyme inhibitor, ramipril, on cardiovascular events in high-risk patients. The Heart Outcomes Prevention Evaluation Study Investigators. *N Engl J Med*. 2000;342:145-53.

124. Cohn JN, Tognoni G and Valsartan Heart Failure Trial I. A randomized trial of the angiotensin-receptor blocker valsartan in chronic heart failure. *N Engl J Med*. 2001;345:1667-75.

125. Hunt SA, Baker DW, Chin MH, Cinquegrani MP, Feldman AM, Francis GS, Ganiats TG, Goldstein S, Gregoratos G, Jessup ML, Noble RJ, Packer M, Silver MA, Stevenson LW, Gibbons RJ, Antman EM, Alpert JS, Faxon DP, Fuster V, Jacobs AK, Hiratzka LF, Russell RO, Smith SC, Jr. and American College of Cardiology/American Heart A. ACC/AHA guidelines for the evaluation and management of chronic heart failure in the adult: executive summary. A report of the American College of Cardiology/American Heart Association Task Force on Practice Guidelines (Committee to revise the 1995 Guidelines for the Evaluation and Management of Heart Failure). *J Am Coll Cardiol*. 2001;38:2101-13.

126. Bohm M and Maack C. Treatment of heart failure with beta-blockers. Mechanisms and results. *Basic Res Cardiol*. 2000;95 Suppl 1:I15-24.

127. Hiona A, Lee AS, Nagendran J, Xie X, Connolly AJ, Robbins RC and Wu JC. Pretreatment with angiotensin-converting enzyme inhibitor improves doxorubicin-

induced cardiomyopathy via preservation of mitochondrial function. *J Thorac Cardiovasc Surg*. 2011;142:396-403 e3.

128. Abd El-Aziz MA, Othman AI, Amer M and El-Missiry MA. Potential protective role of angiotensin-converting enzyme inhibitors captopril and enalapril against adriamycin-induced acute cardiac and hepatic toxicity in rats. *J Appl Toxicol*. 2001;21:469-73.

129. Bosch X, Rovira M, Sitges M, Domenech A, Ortiz-Perez JT, de Caralt TM, Morales-Ruiz M, Perea RJ, Monzo M and Esteve J. Enalapril and carvedilol for preventing chemotherapy-induced left ventricular systolic dysfunction in patients with malignant hemopathies: the OVERCOME trial (preventiOn of left Ventricular dysfunction with Enalapril and caRvedilol in patients submitted to intensive ChemOtherapy for the treatment of Malignant hEmopathies). *J Am Coll Cardiol*. 2013;61:2355-62.

130. Guo YS, Wang CX, Cao J, Gao JL, Zou X, Ren YH and Fan L. Antioxidant and lipid-regulating effects of probucol combined with atorvastatin in patients with acute coronary syndrome. *J Thorac Dis*. 2015;7:368-75.

131. Siveski-Iliskovic N, Kaul N and Singal PK. Probucol promotes endogenous antioxidants and provides protection against adriamycin-induced cardiomyopathy in rats. *Circulation*. 1994;89:2829-35.

132. Bristow MR, Mason JW, Billingham ME and Daniels JR. Doxorubicin cardiomyopathy: evaluation by phonocardiography, endomyocardial biopsy, and cardiac catheterization. *Ann Intern Med*. 1978;88:168-75.

133. Ewer MS, Vooletich MT, Durand JB, Woods ML, Davis JR, Valero V and Lenihan DJ. Reversibility of trastuzumab-related cardiotoxicity: new insights based on clinical course and response to medical treatment. *J Clin Oncol*. 2005;23:7820-6.

134. Campos EC, O'Connell JL, Malvestio LM, Romano MM, Ramos SG, Celes MR, Prado CM, Simoes MV and Rossi MA. Calpain-mediated dystrophin disruption may be a potential structural culprit behind chronic doxorubicin-induced cardiomyopathy. *Eur J Pharmacol*. 2011;670:541-53.

135. Huang RP, Hossain MZ, Huang R, Gano J, Fan Y and Boynton AL. Connexin 43 (cx43) enhances chemotherapy-induced apoptosis in human glioblastoma cells. *Int J Cancer*. 2001;92:130-8.

136. Danialou G, Comtois AS, Dudley R, Karpati G, Vincent G, Des Rosiers C and Petrof BJ. Dystrophin-deficient cardiomyocytes are abnormally vulnerable to mechanical stress-induced contractile failure and injury. *FASEB J*. 2001;15:1655-7.

137. Kostin S, Scholz D, Shimada T, Maeno Y, Mollnau H, Hein S and Schaper J. The internal and external protein scaffold of the T-tubular system in cardiomyocytes. *Cell Tissue Res*. 1998;294:449-60.

138. Schaper J, Froede R, Hein S, Buck A, Hashizume H, Speiser B, Friedl A and Bleese N. Impairment of the myocardial ultrastructure and changes of the cytoskeleton in dilated cardiomyopathy. *Circulation*. 1991;83:504-14.

139. Doroshow JH and Davies KJ. Redox cycling of anthracyclines by cardiac mitochondria. II. Formation of superoxide anion, hydrogen peroxide, and hydroxyl radical. *J Biol Chem*. 1986;261:3068-74.

140. Pacher P, Beckman JS and Liaudet L. Nitric oxide and peroxynitrite in health and disease. *Physiol Rev*. 2007;87:315-424.

141. Mukhopadhyay P, Rajesh M, Batkai S, Kashiwaya Y, Hasko G, Liaudet L, Szabo C and Pacher P. Role of superoxide, nitric oxide, and peroxynitrite in doxorubicin-induced cell death in vivo and in vitro. *Am J Physiol Heart Circ Physiol*. 2009;296:H1466-83.

142. Thomas A, Lenglet S, Chaurand P, Deglon J, Mangin P, Mach F, Steffens S, Wolfender JL and Staub C. Mass spectrometry for the evaluation of cardiovascular diseases based on proteomics and lipidomics. *Thromb Haemost*. 2011;106:20-33.

143. Puri R, Duong M, Uno K, Kataoka Y and Nicholls SJ. The emerging role of plasma lipidomics in cardiovascular drug discovery. *Expert Opin Drug Discov*. 2012;7:63-72.

144. Bochkov VN, Oskolkova OV, Birukov KG, Levonen AL, Binder CJ and Stockl J. Generation and biological activities of oxidized phospholipids. *Antioxid Redox Signal*. 2010;12:1009-59.

145. Sharov VG, Sabbah HN, Shimoyama H, Goussev AV, Lesch M and Goldstein S. Evidence of cardiocyte apoptosis in myocardium of dogs with chronic heart failure. *Am J Pathol*. 1996;148:141-9.

146. Saraste A, Pulkki K, Kallajoki M, Henriksen K, Parvinen M and Voipio-Pulkki LM. Apoptosis in human acute myocardial infarction. *Circulation*. 1997;95:320-3.

147. Wu S, Ko YS, Teng MS, Ko YL, Hsu LA, Hsueh C, Chou YY, Liew CC and Lee YS. Adriamycin-induced cardiomyocyte and endothelial cell apoptosis: in vitro and in vivo studies. *J Mol Cell Cardiol*. 2002;34:1595-607.

148. Kumar D, Kirshenbaum L, Li T, Danelisen I and Singal P. Apoptosis in isolated adult cardiomyocytes exposed to adriamycin. *Ann N Y Acad Sci*. 1999;874:156-68.

149. Zhang YW, Shi J, Li YJ and Wei L. Cardiomyocyte death in doxorubicin-induced cardiotoxicity. *Arch Immunol Ther Exp (Warsz)*. 2009;57:435-45.

150. Kobayashi S, Volden P, Timm D, Mao K, Xu X and Liang Q. Transcription factor GATA4 inhibits doxorubicin-induced autophagy and cardiomyocyte death. *J Biol Chem*. 2010;285:793-804.

151. Zhang Y, Kang YM, Tian C, Zeng Y, Jia LX, Ma X, Du J and Li HH. Overexpression of Nrdp1 in the heart exacerbates doxorubicin-induced cardiac dysfunction in mice. *PLoS One*. 2011;6:e21104.

152. Ryter SW, Kim HP, Hoetzel A, Park JW, Nakahira K, Wang X and Choi AM. Mechanisms of cell death in oxidative stress. *Antioxid Redox Signal*. 2007;9:49-89.